1

Rapid #: -2402297

Ariel
IP: 128.210.125.135

Status	Rapid Code	Branch Name	Start Date
Pending	UUE	Eccles Library	3/13/2009 8:29:16 AM

CALL #: **Journals**
LOCATION: **UUE :: Eccles Library :: Eccles Library**

TYPE:	Article CC:CCL
JOURNAL TITLE:	Journal of parenteral science and technology
USER JOURNAL TITLE:	Journal of Parenteral Science and Technology
UUE CATALOG TITLE:	Journal of parenteral science and technology : a publication of the Parenteral Drug Association
ARTICLE TITLE:	Use of Laboratory Data in Freeze Drying Process Design: Heatand Mass Transfer Coefficients and the Computer Simulation of FreezeDrying
ARTICLE AUTHOR:	Pikal, M.J.
VOLUME:	39
ISSUE:	
MONTH:	
YEAR:	1985
PAGES:	115-138
ISSN:	0279-7976
OCLC #:	
CROSS REFERENCE ID:	789905
VERIFIED:	

pwm

BORROWER: **IPL :: Main Library**
PATRON: **Mockus,Linas**

PATRON ID:	-
PATRON ADDRESS:	-
PATRON PHONE:	-
PATRON FAX:	-
PATRON E-MAIL:	-
PATRON DEPT:	
PATRON STATUS:	Staff
PATRON NOTES:	-

The following paper was part of a Symposium on Lyophilization presented at the Annual Meeting of the Academy of Pharmaceutical Sciences, San Diego, California, 1982

Use of Laboratory Data in Freeze Drying Process Design: Heat and Mass Transfer Coefficients and the Computer Simulation of Freeze Drying

M. J. PIKAL

Lilly Research Laboratories, Indianapolis, Indiana

ABSTRACT: Freeze drying process development normally proceeds via an empirical "trial and error" experimental approach which is both time consuming and uncertain in reliable extrapolation to production equipment. This research describes the use of phenomenological theory, with key parameters determined by laboratory experiments, to guide the experimental program to optimize the primary drying stage of the process for a given product/container combination. The theoretical description of primary drying is a problem in coupled heat and mass transfer which can be satisfactorily described using a steady-state model where the heat flow is given by the product of the mass flow and the heat of sublimation. Generally, mass transfer is impeded by three barriers or resistances: resistance of the dried product layer, resistance of the semi-stoppered vial, and resistance of the chamber. Resistance, defined as a ratio of pressure difference to mass flow, is experimentally determined for each barrier. The resistance of the dried product normally increases with time as the thickness of dried product increases and typically accounts for over 90% of the total resistance to mass transfer. Heat flow from the shelf surface to the subliming ice is impeded by three barriers: the interface between the shelf surface and the bottom of the tray used to contain the vials, the interface between the tray and the vial bottom, and the ice between the bottom of the vial and the sublimation surface. Heat flow is described in terms of heat transfer coefficients, defined as the ratio of the heat flux to temperature difference, where the heat transfer coefficients are experimentally determined for each vial and tray of interest. Vial and tray heat transfer coefficients increase with increasing pressure and are quite sensitive to variations in degree of flatness of the vial or tray bottom. Steady-state transport theory is used to define six equations with eight variables where the equations contain mass transfer resistances and heat transfer coefficients which are determined from laboratory experiments. The variables are the sublimation rate and the pressures and temperatures throughout the system. Our procedure is to fix two of the variables (i.e., chamber pressure and shelf temperature) and solve, via a computer program, for the other six variables. Solutions are obtained for 0, 20, 40, 60, 80, and 100% completion of primary drying, thereby providing sublimation rate and the relevant temperatures and pressures as a function of time during the freeze-drying cycle defined by the input parameters chosen (i.e., the chamber pressure and shelf temperature profile with time). Thus, computer-generated freeze-drying cycles may be generated for any combination of product, container, and process parameters desired. Agreement between theoretical and experimental cycles is satisfactory. Use of this approach is demonstrated with the following applications: (1) a study of the effect of changes in chamber pressure and shelf temperature on drying time and product temperature; (2) the effect of shelf temperature variability and vial heat transfer coefficient variability on uniformity of drying; and (3) cycle optimization.

Freeze-drying, or lyophilization, has several advantages over competing processes for the production of pharmaceuticals. First, since freeze-drying is a low temperature process, chemical decomposition may be minimized. Second, since the solution may be sterile-filtered immediately before filling into a vial and no powder handling steps are involved in subsequent processing, particulate levels may be reduced to a minimum. However, since process times are often long and capital equipment costs are high, freeze drying is frequently regarded as an expensive process, and there is considerable economic motivation to minimize process times (1). Indeed, the objective of freeze-drying process development is to minimize the process time while maintaining high product quality. In-process decomposition must be minimized, the residual water content of the product frequently must be low to enhance shelf life of the product (2), and the "foaming" or "puffing" that accompanies eutectic melt or collapse must be avoided to maintain product elegance.

The freeze-drying process may be divided into three stages: freezing, primary drying or ice sublimation, and secondary drying or water desorption. Details of the

Received November 26, 1983. Accepted for publication March 1, 1984.

freezing process influence the structure of the porous solid product remaining after ice removal and therefore, may strongly influence the time required to complete the next two stages as well as the properties of the final product (1, 3, 4). Secondary drying is the removal of absorbed or hydrate water. Optimization of this stage requires information on the effect of temperature on both in process decomposition rate and drying rate. It should be noted that if both rates have the same activation energy, the amount of decomposition produced in achieving a fixed residual water level is independent of drying temperature (5). The primary drying stage, normally the most time-consuming portion of the process, is the subject of this report. The duration of primary drying is reduced sharply by increasing the product temperature, but to avoid collapse or eutectic melt, this stage must be carried out below the maximum allowable product temperature (eutectic temperature for a crystalline solute or collapse temperature for an amorphous solute). Clearly, determination of the maximum allowable product temperature is of extreme importance and is the first step in process development. Collapse and eutectic temperatures may be determined by thermal analysis methods (6, 7), electrical resistance measurements (8), and by direct microscopic observation of freeze drying as a function of temperature (4, 9). In our view, the microscopic technique is the method of choice for collapse temperature determination simply because one actually *observes* the structural collapse, thereby removing any ambiguity due to data interpretation.

Once the maximum allowable product temperature is known, the primary drying stage is optimized by determining the shelf temperature and chamber pressure time sequence required to maintain the product temperature *slightly* lower than the maximum allowable temperature during all of primary drying. The shelf temperature/chamber pressure vs. time relationship is normally determined by an empirical "trial and error" experimental approach which is both time-consuming and uncertain in reliable extrapolation to production equipment. In practice, due to the development time required to truly optimize primary drying, many freeze-drying processes are not optimized. Rather, a process is developed which yields material of acceptable quality but only minimal attention is given to optimization. Worse yet, there is a temptation to assume that a process which is acceptable for a given product in one dose/container combination will also be acceptable for another dose/container combination with only an adjustment in process time.

Optimization of the shelf temperature/chamber pressure vs. time relationship is a problem in coupled mass and heat transfer. This research describes the use of mass and heat transfer theory to first define key heat and mass transfer coefficients that may be determined by laboratory experiments, followed by a computer-assisted theoretical analysis which allows pressures, temperatures, and freeze-drying rates to be calculated for any proposed process with any product/container combination. Once the basic data set describing the heat and mass transfer characteristics of the freeze dryers and containers of interest is available, either by measurement or estimation, the mass transfer coefficient of the product is the only additional information needed to fully characterize primary drying of that product in any container using any proposed shelf temperature/chamber pressure vs. time program. Thus, much of the experimental effort in optimizing the primary drying stage may be replaced by "computer-simulated freeze drying."

Like many of the previous theoretical treatments of freeze drying (10–15), our development is based on a combination of nonequilibrium thermodynamics (16) and kinetic theory of gases (17). An approximate nonequilibrium thermodynamics formalism is used where cross-terms representing, for example, the effect of temperature gradients on mass transfer are not explicitly included. Thus, while less rigorous than several other treatments (12, 13), omission of the cross-terms is not expected to introduce significant error (14, 15), and the resulting simplification is of significant advantage when theoretical calculations are carried out on practical problems in freeze drying. Moreover, since heat and mass transfer coefficients are defined using the same theoretical formalism, and are then experimentally measured, contributions of cross-terms will be implicitly included, to some extent, in the measured coefficients.

Except for a time dependence in the thickness of dried product which forms above the receding ice-vapor boundary, the theoretical model assumes steady-state heat and mass transfer. Such pseudo steady-state models, with a moving planar boundary, have been employed by other workers (10, 14, 15) and may be justified as an excellent approximation over most of primary drying by theoretical arguments (15) and by experimental observation. For example, since the volume flow rate to system volume ratio is so large, one observes that step changes in chamber pressure produce corresponding changes in pressure in other parts of the freeze-drying system on an instantaneous basis. Temperature response is much slower but the rapid changes in product temperature following a step change in shelf temperature usually dissipates within 15–30 min leaving only the small time dependence in temperature due to the moving boundary. Thus, pseudo steady state is normally achieved within 30 min after a change in shelf temperature. The heat flow may be divided into two contributions: (*1*) the heat flow required to change the system temperature, given by the product of the rate of temperature change and the system heat capacity, and (*2*) the heat flow required to sublime the ice, given by the product of the sublimation rate and the heat of sublimation. The theoretical model employed in the present studies assumes all heat flow is used to sublime ice. In pseudo steady state, this simplifying approximation is normally accurate within about 1% in heat transfer rate and is an entirely satisfactory approximation for the purposes of this study.

Nearly all of the previous theoretical treatments of freeze drying have been directed at applications in the food industry. Because of significant differences between the freeze drying of food products and pharmaceuticals, these studies have only limited validity for the pharmaceutical industry. Normally, the heat supply for freeze-drying foods is accomplished by radiative heating of the dried product and subsequent conduction through the dried product to the

subliming ice. Pharmaceuticals are normally freeze dried in vials where heat is supplied from the shelf to the vial bottom by a combination of mechanisms (18, 19). Heat flow from the vial bottom to the sublimation interface proceeds by conduction through the frozen product. Second, foods are frequently processed at much higher chamber pressures, presumably to maximize heat transfer without scorching the dried product, which has led some theoreticians to assume mass transfer proceeds via diffusion of water vapor in air. While this assumption may be generally valid for food processing, pharmaceutical products are normally freeze dried at much lower chamber pressures where experimentally it is found (19) that the gas present in both the vial and the drying chamber is mostly water vapor. Thus, particularly in the dried product layer where the gas is typically over 90% water vapor (19), the gas is essentially a one component system and diffusion is negligible. Vapor transport in the dried product layer, which normally accounts for about 90% of the resistance to mass transfer (19) proceeds by Knudsen flow (4, 19) while flow through the semi-stoppered vial and flow from the drying chamber to the condenser proceeds by both Knudsen flow and hydrodynamic or viscous flow (19). Several recent modeling studies of pharmaceutical freeze drying (15, 20) do recognize the importance of Knudsen flow. Since the details of the theoretical model used are not given in the study by Cise (20), a comparison with this report is not possible. The theoretical model developed by Litchfield and Liapis (15) differs from our analysis in several important details. First, the heat and mass transfer coefficients used by Litchfield and Liapis are inconsistent with recent experimental findings (4, 19), and second, Litchfield and Liapis (15) arbitrarily fixed the mole fraction of water inside the vial at values significantly less than unity by imposing a boundary condition. Thus, their calculations refer to a hypothetical system which is not normally encountered in pharmaceutical freeze drying (19).

The theoretical model employed in this report is a pseudo steady-state transport model where the transport coefficients are evaluated by laboratory experiments (4, 19) under conditions relevant to the conditions commonly used in production-scale processing of pharmaceuticals. This report is divided into three main sections: (*1*) the definition and measurement of heat and mass transfer coefficients is discussed, and some representative results are given; (*2*) the theoretical model which relates sublimation rate and product temperature to process and formulation variables is presented. The computer-assisted solution of the resulting set of equations is described, and a comparison of theoretical and experimental results is presented to justify the accuracy of the theoretical model; and (*3*) the use of the theoretical model in process design is illustrated by a study of the effect of changes in chamber pressure and shelf temperature on drying time and product temperature, by studies of the effect of shelf temperature variability and vial heat transfer coefficient variability on uniformity of drying, and by several examples of cycle optimization studies.

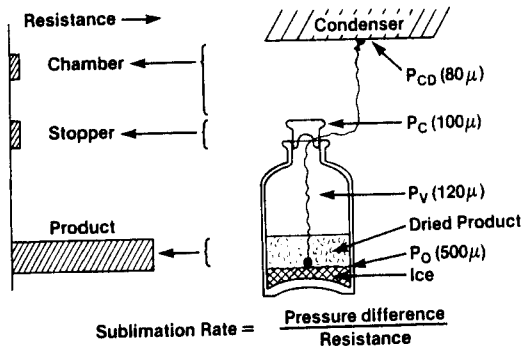

Figure 1—Mass transfer in primary drying: schematic of resistances.

1. Transport Coefficients: Definition, Measurement, and Results

1.1 Mass Transfer Coefficients

1.11 Definition of Mass Transfer Coefficients: Mass transfer is discussed in terms of resistance, defined as the ratio of the driving force across the barrier (pressure difference) to the mass flow through the barrier. Resistance, rather than permeability (the reciprocal of resistance) is used since the total resistance is additive for several component resistances in series. In passing from the frozen product to the condenser, the flow of water vapor is impeded by three main barriers or resistances (Fig. 1). A frozen solution dries from the top, thereby producing a dried-product layer above the ice which increases in thickness as sublimation proceeds. The dried product, a porous solid, imposes a resistance to mass transfer and a corresponding pressure drop across the dried product layer (Fig. 1). The stopper, in the semi-stoppered configuration, has one or more small openings to allow for vapor flow and also contributes a resistance to mass transport and a corresponding pressure drop (Fig. 1). Likewise, due to the resistance of the chamber to condenser pathway, a small pressure drop exists between the drying chamber and the condenser chamber. The bar graph on the left of Figure 1 gives the relative contributions of the components of resistance for a typical freeze-drying system. Note that the dried product resistance is by far the largest barrier to mass flow.

Although not shown in Figure 1, a condenser resistance may be associated with the process of conversion of water vapor in the condenser chamber to ice on the condensers, yielding a water partial pressure inside the condenser chamber significantly larger than the vapor pressure of ice on the condenser surface. Preliminary experimental observations (21) indicate that the condenser resistance is quite small but increases in direct proportion to the partial pressure of air in the condenser chamber. Under the "typical" conditions shown in Figure 1, the condenser resistance is about a factor of ten less than the chamber resistance.

When the mean-free path is large compared to the dimensions of the pores or tubes constituting the physical system responsible for resistance to vapor flow, as is the case with vapor flow through a dried product (4), collisions of water molecules with the pore or tube walls are responsible for resistance to vapor flow, and the flow mechanism is said to be free molecular or Knudsen flow (17). Here, the driving

force is simply the difference in partial pressure of water (14, 17), although the difference in total pressure could be used as well. That is, in the Knudsen flow region, the consequence of zero net flow of inert gas (air) is a zero gradient of air pressure across the barrier (i.e., the dried product). Note that the driving force for the phase change (sublimation) at the ice-vapor interface is the difference between the equilibrium vapor pressure of ice and the partial pressure of water at the ice-vapor interface. Thus, the resistance of the dried product layer, R_p, is defined by

$$R_p = (P_0 - X_1^v P_v)/\dot{m}, \qquad \text{(Eq. 1)}$$

where P_0 is the equilibrium vapor pressure of the subliming ice in mmHg, X_1^v is the mole fraction of water vapor in the vial, P_v is the total pressure in the vial in mmHg, and $\dot{m}$ is in the sublimation rate in ghr^{-1} per vial. As defined, R_p includes both the resistance for the phase change at the ice-vapor interface and the resistance corresponding to the mass transfer of water through the dried product layer above the ice-vapor interface. Except for frozen systems of extremely low solids content, the relative contribution of the phase change resistance is negligible (4). The dried product resistance depends on the geometric cross-sectional area of the product normal to the direction of water flow, A_p,

$$R_p = \hat{R}_p/A_p, \qquad \text{(Eq. 2)}$$

where $\hat{R}_p$ is the area normalized product resistance, denoted "normalized product resistance," which is independent of sample area but depends on both the nature of the product and the thickness of the dried product layer. Thus, the product resistance, R_p, depends on the container used in that A_p is fixed by the internal diameter of the vial.

When the mean-free path is small compared to pore or tube dimensions, collisions between gas molecules are much more frequent than collisions of gas molecules with pore walls, and the resistance is due to momentum transfer between gas molecules, or viscous "forces." Here, the flow mechanism is "viscous flow" (17), and the driving force is the difference in total pressure (Poiseuille's Law). The distinction between partial pressure and total pressure is obviously not important when the gas phase is essentially pure water, as indeed is the case in the vial and drying chamber during primary drying under most conditions of practical interest (9).

For flow of water vapor from the vial interior to the chamber, the mean-free path may be of the same order of magnitude as the openings in the semi-stoppered container. In such cases, both Knudsen flow and viscous flow mechanisms are involved in mass transfer, and the flow mechanism is referred to as "transition flow" (17). It should be noted that the net flow of air from the vial interior to the chamber is zero, although the pressure gradient of air is not necessarily zero in transition flow. Manipulation of mass transfer equations presented by Liapis and Litchfield (Eqs. 11 and 12 in Ref. 14) indicate that the difference in total pressure is the most appropriate driving force for transition flow of water vapor with zero net flow of air. That is, with the difference in total pressure as the driving force, the resistance is essentially independent of vapor composition and varies with total pressure in simple fashion. Thus, the stopper resistance, R_s, is defined by

$$R_s = (P_v - P_c)/\dot{m}, \qquad \text{(Eq. 3)}$$

where P_c is the total chamber pressure (mmHg). If there is an additional mass transfer barrier between the vial interior and the drying chamber, such as a tray lid, the pressure difference in Eq. 3 becomes, $P_v - P_{tr}$, where P_{tr} is the pressure in the immediate area of the vial exterior (tray pressure). The tray resistance per vial, R_{tr} is then defined by

$$R_{tr} = (P_{tr} - P_c)/n\dot{m}, \qquad \text{(Eq. 4)}$$

where n is the number of vials per tray.

Since a controlled leak of inert gas (air or nitrogen) is frequently introduced into the drying chamber to control the heat transfer rate, the flow of air from the drying chamber to the condenser chamber is not identically zero. However, in the usual freeze drying system, the pumping speed for condensables (H_2O) is vastly greater than the pumping speed for air, and the flow rate of air *relative* to the flow rate of water is approximately zero. Thus, the resistance of the drying chamber to condenser chamber pathway, denoted chamber resistance, R_c, is defined in terms of a difference in total pressure between the drying chamber, P_c, and condenser chamber, P_{cd},

$$R_c = (P_c - P_{cd})/N\dot{m}, \qquad \text{(Eq. 5)}$$

where N is the total number of vials in the dryer.

The stopper, tray, and chamber resistances defined here should be pressure dependent and, when the vapor is pure water, are expected (17) to be of the form,

$$R_i^{-1} = a_0 + a_1\overline{P}_i,\ i = s, tr, c, \qquad \text{(Eq. 6)}$$

where R_i refers to R_s, R_{tr}, or R_c, and $\overline{P}_i$ is the mean pressure across the barrier. For example, for $i = s$ and no tray lid, $\overline{P}_s = (P_v + P_c)/2$. A derivation based on mass transfer theory (Eqs. 11 and 12 in Ref. 14) demonstrates that even when the mole fraction of water vapor is not unity, Eq. 6 should be an excellent approximation in any system where the molar flow rate of air is small compared to the molar flow rate of water vapor.

Since the driving force for the condensation of water vapor on the condensers is the difference between the partial pressure of water vapor and the equilibrium vapor pressure of ice at the condenser ice/vapor boundary, the condenser resistance, R_{cd}, is defined by

$$R_{cd} = (P_1^{cd} - P_1^s)/\dot{m}N, \qquad \text{(Eq. 7)}$$

where P_1^{cd} is the partial pressure of water vapor in the condenser chamber, and P_1^s is the equilibrium vapor pressure of ice at the surface temperature of the condenser ice.

With the approximation $X_1^v = 1$, combination of Eqs. 1–7 gives,

$$\dot{m} = R_T^{-1}(P_0 - P_2^{cd} - P_1^s), \qquad \text{(Eq. 8)}$$

where P_2^{cd} is the partial pressure of inert gas in the condenser chamber, and R_T is the total resistance,

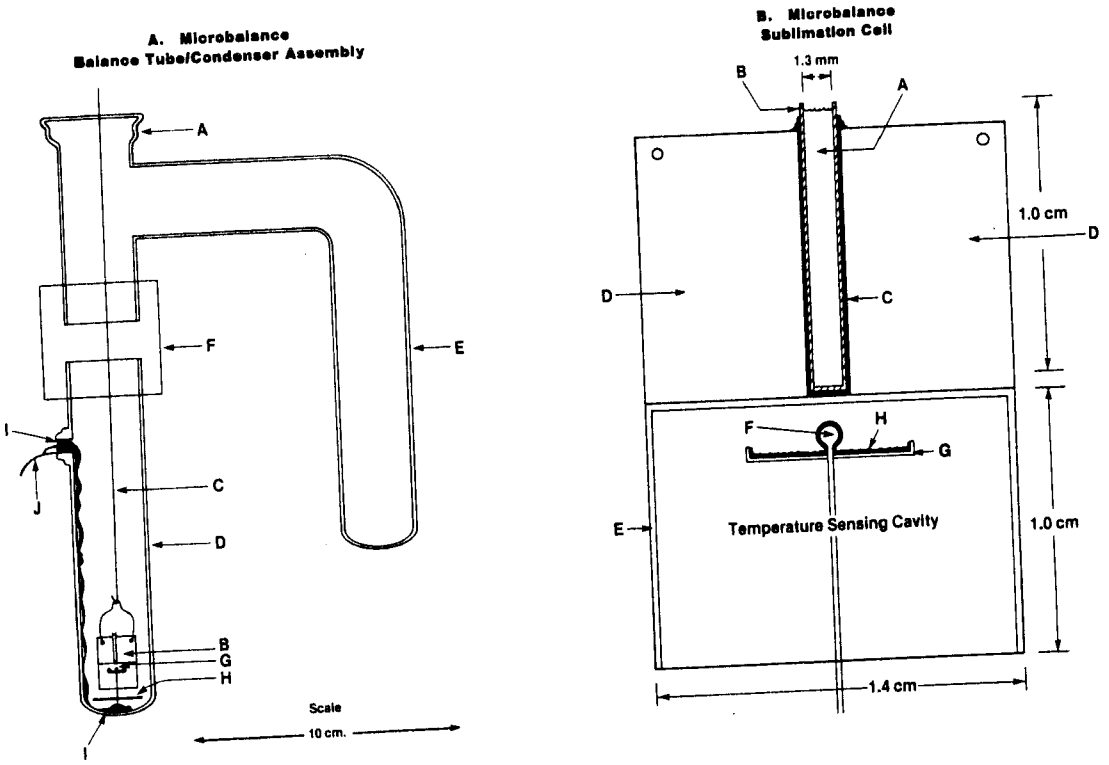

Figure 2—Microbalance sublimation apparatus.

$$R_T = R_p + R_s + nR_{tr} + NR_c + NR_{cd}, \quad \text{(Eq. 9)}$$

under normal operating conditions, P_1^s is negligibly small, and the net driving force is the difference between the equilibrium vapor pressure of ice at the sublimation interface, P_0, and the partial pressure of air in the condenser chamber, P_2^{cd}. The quantities, nR_{tr}, NR_c, and NR_{cd} are denoted "scaled" resistances. A scaled resistance is, in effect, the resistance of the barrier per vial.

1.12 Measurement of Dried Product Resistance: Microbalance Technique: "Apparatus"—This methodology (4) is based upon determining the sublimation rate of a frozen microsample with a recording high vacuum microbalance and is an extension of the procedure used by MacKenzie and Luyet (22). The sample cell is designed to be more convenient in use and the design permits resistance data to be obtained at higher temperatures (*c.a.* −10°) and for dried product thicknesses up to 1 cm. The sample is contained in a 1.3-mm diameter glass tube which, in turn, is imbedded in an aluminum heat exchanger which allows isothermal operation at the temperature of the thermostat for most systems of interest. The sample is suspended from one arm of an electronic vacuum microbalance which is connected to a high vacuum line. The sublimation cell, or sample holder, is enclosed by a balance tube/condenser assembly (Fig. 2*A*) which is connected to the balance via a glass "0" ring joint (*A*). The sublimation cell (*B*) is suspended from the balance beam by a 0.25-mm diameter nichrome wire (*C*). During operation, the glass balance tube (*D*) is immersed in a thermostat, and the glass side arm tube (*E*) is immersed in dry ice/acetone to serve as the condenser. A high vacuum union (*F*) allows rapid connection of the balance tube to the rest of the assembly. A copper-constantan thermocouple probe (*G*) fits inside a cylindrical cavity formed by the bottom portion of the sublimation cell. A circular aluminum foil heat shield (*H*) is intended to isolate the thermocouple probe from thermal radiation coming from the bottom of the sample tube. High vacuum wax (*I*) is used to seal the thermocouple wires (*J*) to the sample tube, to form a vacuum seal at the point where the wires exit the sample tube and to support the thermocouple probe in fixed position at the bottom of the balance tube.

A critical aspect of the sublimation rate experiment is the ability to control and measure the sample temperature. The sublimation cell (Fig. 2*B*) is essentially a glass capillary tube in good thermal contact with an efficient radiative heat exchanger. This design allows the heat required for sublimation to be transferred from the thermostat to the sample with minimal temperature gradients. The sample (*A*) is in a glass capillary tube (*B*) which is "glued" into a cylindrical hole in the aluminum heat exchanger by a thin film of high vacuum wax (*C*). To maximize radiative heat transfer, the aluminum is given a black anodized finish. The top portion of the heat exchanger has four "fins" (*D*) at 90° with respect to each other while the bottom portion (*E*) is a cylindrical cavity termed the temperature sensing cavity. The thermocouple probe protrudes into this cavity without touching the sublimation cell. To increase the efficiency of heat exchange between the thermocouple probe and the sublimation cell, the effective area of the thermocouple probe is increased by "gluing" the thermocouple junction (*E*) to an aluminum disk (*G*) with a thin coat of high vacuum wax (*H*).

Ideally, the probe measures the cell temperature which is identical to the sample temperature. In practice, the probe temperature does not exactly measure the cell temperature, and at high sublimation rates, the sample temperature is

slightly lower than the cell temperature. However, the sample temperature may easily be calculated from the measured probe temperature and sublimation rate (4).

The rate of mass loss computed (by numerical differentiation) from the recorder mass vs. time curve is corrected for background effects (4) to obtain the sublimation rate, $\dot{m}$. The sample temperature is used to calculate the vapor pressure of subliming ice, P_0, while the partial pressure of water vapor above the dried product is essentially zero (4). Thus, the normalized product resistance, $\hat{R}_p$, is evaluated from the raw data using Eqs. 1 and 2, where the product area, A_p, is evaluated from the capillary tube cross-sectional area. The thickness of the dried product, denoted, l, is evaluated from,

$$l = \frac{mo - m(t)}{\rho_I A_p \epsilon}, \qquad \text{(Eq. 10)}$$

where mo is the initial samples mass, $m(t)$ is the mass remaining at time t, ρ_I is the density of ice, and ϵ is the porosity of volume fraction of ice. Equation 10 assumes that the ice-vapor boundary remains planar and normal to the axis of the cylindrical container (i.e., the capillary tube) during sublimation, a very good approximation for microbalance freeze drying (4).

"Representative Results"—Theoretical models in common use (11, 15, 23) assume the equivalent of $\hat{R}_p \propto l$, which results in the quantity of ice being sublimed being directly proportional to the square root of time (11, 23). Essentially four classes of $\hat{R}_p$ dependence of l have been observed (4), none of which correspond to the simple proportionality to l (Fig. 3). All data show a non-zero intercept at $l = 0$, and the dependence of $\hat{R}_p$ on l is frequently nonlinear. The variation of normalized product resistance, $\hat{R}_p$, with thickness of dried product, l, is well represented by the empirical equations,

$$\hat{R}_p = R_p(0), 0 \le l \le l', \qquad \text{(Eq. 11)}$$

$$\hat{R}_p = R_0 + A_1 l/(1 + A_2 l), l' \le l, \qquad \text{(Eq. 12)}$$

where $l' = 0$ (and therefore, $\hat{R}_p(0) = R_0$) for most systems studied. The parameters $\hat{R}_p(0)$, R_0, A_1, and A_2 are "constants" determined by regression analysis of the raw data. Type I curves (Fig. 3) show a linear dependence of $\hat{R}_p$ on l throughout the l range studied. A Type II curve exhibits a sharp decrease in $\hat{R}_p$ at low l, followed by a linear increase in $\hat{R}_p$ with increasing l for $l > 0.2$ cm. With a Type II curve, $\hat{R}_p(0) > R_0$. Type III and Type IV curves are concave toward the l axis, the curvature being slight for Type III curves but severe for Type IV. The observation that $R_p(0)$ is significantly larger than zero suggests the presence of a surface barrier resulting from a different structure for the dried product near the surface (4). The surface barrier for Type II curves appears to be a high resistance amorphous skin which, after some water desorption, cracks and decreases in effective resistance (4).

In general, the dried product resistance increases as the concentration of solute increases, although for some amorphous systems, the concentration dependence is slight. For example, the increase in resistance is roughly proportional to volume percent solid for potassium chloride systems, while for povidone, the resistance is nearly independent of solute concentration between 10% (v/v) and 23% (v/v) (4).

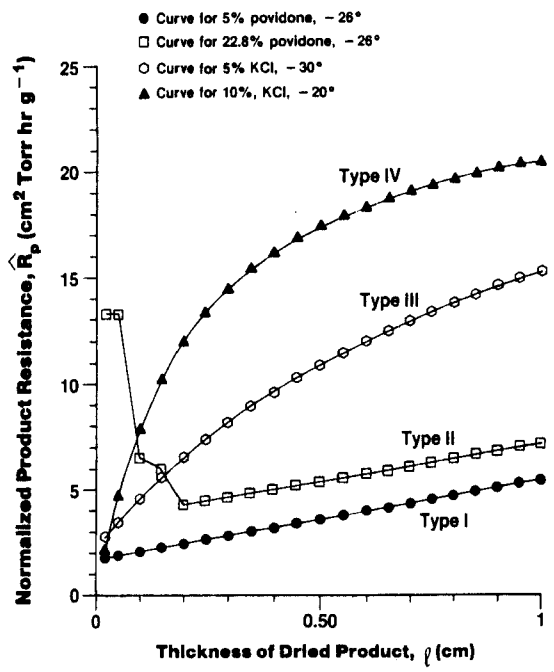

Figure 3—Dependence of product resistance on dried product thickness: types of behavior.

The usual theoretical models (11, 17, 23, 24) describing gas flow result in a dried product resistance which is essentially independent of temperature. However, experimental results demonstrate a very significant temperature effect. For most systems studied to date (4, 25), the dried product resistance at larger l values *decreases* significantly as the temperature approaches the eutectic temperature (or collapse temperature for an amorphous solute), a result attributed (4) to the emergence of hydrodynamic surface flow of adsorbed water as an additional flow mechanism for transport of water at higher temperature.

1.13 Measurement of Dried Product Resistance: Vial Technique: "Apparatus"—Vial freeze drying is carried out in a highly modified commercial laboratory freeze dryer (4, 19). The freeze dryer is equipped with a temperature-controlled shelf, thermocouple measurement of shelf and product temperature and pressure measurement in the sample chamber and inside one of the vials. Pressure inside a vial is measured by connecting a glass tube to the interior of the vial at a location between the vial neck and the top surface of the product. This tube is joined to another tube which leads out of the vacuum chamber to the vial pressure sensor. Vial pressure, chamber pressure, and all thermocouple outputs are displayed as a function of time by a 24-channel recorder. The pressure sensors are differential capacitance manometers and measure absolute pressure, independent of vapor composition.

Calculation of the resistance of the dried product requires the following data:

(1) The vapor pressure of subliming ice, which may be evaluated from the product temperature data;
(2) The partial pressure of water vapor in the vial, which

to an excellent approximation is equal to the total pressure in the vial;

(3) The area of the product, which is calculated from the vial dimensions; and

(4) The sublimation rate.

Since the apparatus does not allow the mass of the vial to be continuously monitored, the sublimation rate is evaluated by an alternate procedure, which essentially uses the stopper as a "flow-meter." The sublimation rate is related to the stopper resistance and the pressure difference across the stopper (Eq. 3), where the stopper resistance depends on pressure through Eq. 6. Since the viscous flow mechanism normally predominates, and since the variation in $\overline{P}$ during a given experiment is slight, the sublimation rate for a given experiment may be characterized by a single mass transfer coefficient $\overline{R}_s$ (4), defined by,

$$\dot{m} = \overline{R}_s^{-1}(P_v^2 - P_c^2)/2. \qquad \text{(Eq. 13)}$$

Since the mass of water removed during the experiment, Δm, is easily determined, $\overline{R}_s$ may be evaluated from the integrated form of Eq. 13,

$$\overline{R}_s = \frac{1}{2\Delta m}\int_0^{t_0}(P_v^2 - P_c^2)dt, \qquad \text{(Eq. 14)}$$

where t_0 is the duration of the experiment and the indicated integration is performed numerically. Since slight variations in stopper placement causes variations in $\overline{R}_s$, a value of $\overline{R}_s$ is determined for each experiment. Once $\overline{R}_s$ is determined from Eq. 14, the sublimation rate at any time during the experiment is evaluated from the measured pressure values and Eq. 13. The normalized product resistance is calculated from Eq. 1, and the thickness of the dried product is calculated from Eq. 10, where $mo\text{-}m(t)$ is evaluated by numerical integration of the sublimation rate data. The assumption of a planar ice-vapor boundary, required by Eq. 10, is less satisfactory in vial freeze drying than with microbalance freeze drying but is still a good first approximation.

Due to both the uncertainty in the temperature of subliming ice (±0.8 °C) and the sensitivity of sublimation rate to small errors in pressure measurement, product resistance data determined from vial experiments are much less precise than are corresponding microbalance data. Moreover, due to the time required to establish steady state at the start of a vial experiment, product resistance data cannot be obtained at very low l values.

"Representative Results"—Normalized product resistance data determined by vial and microbalance techniques are in qualitative agreement (4, 25) with regard to variation with dried layer thickness, solute concentration, nature of the solute, and temperature. However, microbalance derived resistances are normally about a factor of two higher than corresponding vial generated data. This result is attributed (4) to the much faster freezing rate, and resulting smaller pore size in the dried product, for microbalance samples. Representative normalized resistance data based upon vial experiments are summarized by Table I where the parameters for Eq. 12 are listed. Equation 12 is a good representation of the resistance data over the entire range of l values studied (0.05–1.3 cm) for all products except DOBUTREX. In qualitative agreement with microbalance data, DOBUTREX appears to exhibit Type II behavior, where $\hat{R}_p(0)$ is about 5.5 for the vial derived data. The temperature dependence in $\hat{R}_p$ may be satisfactorily described by a strong dependence of A_2 on absolute temperature, T. Although the functions chosen (Table I) represent the limited data available and appear consistent with surface transport of water (4), a good deal more experimental and theoretical work is needed to rigorously determine the dependence of $\hat{R}_p$ on temperature.

1.14 Measurement of Closure, Tray, and Chamber Resistance: "Procedures"—Closure or stopper resistance at a given mean pressure, $\overline{P}$, is determined by measuring the average pressure difference across the stopper, in the semi-stoppered position, during sublimation of a known quality of ice at constant chamber pressure. The mean pressure, $\overline{P}$, is the mean of the pressures inside and outside the vial during sublimation, and the mean sublimation rate is calculated from the mass of ice sublimed from that vial and the time of sublimation. The closure resistance is then determined from Eq. 3.

The tray resistance may be determined using basically the same procedure used for closure resistant measurement, provided the pressure inside the tray may be determined. However, production size trays are too large for our laboratory dryer so an alternate procedure utilizing a pilot-scale dryer is used. Here, the average sublimation rate for vials contained in trays with lids is compared with the average sublimation rate for vials in trays without lids in the same experiment. For the vials in trays without lids,

$$R_p + R_s = (P_0 - P_c)/\dot{m}, \qquad \text{(Eq. 15)}$$

while for vials in trays with lids,

$$R_p + R_s' + nR_{tr} = (P_0' - P_c)/\dot{m}', \qquad \text{(Eq. 16)}$$

where the prime symbol denotes a parameter for the "lid on" configuration. The parameters on the right-hand sides of Eqs. 15 and 16 are measured experimentally. Since the

TABLE I Parameters Characterizing Normalized Product Resistance for Selected Products Freeze Dried in Vials

Product	Parameters for Eq. 12		
	R_0	A_1	A_2
KCl, 5% (v/v)	1.22	6.86	$4.45\cdot10^{13}\exp(-8.36\cdot10^3/T)$
DOBUTREX[a]	3.08	10.3	$6.23\cdot10^{13}(1 - T/263.16)^{-7.4}$
Povidone, 5% (v/v)	1.13	5.0	0
Mannitol, 5% (w/w)	1.40	16.0	0

[a] DOBUTREX is Dobutamine Hydrochloride:mannitol in a 1.12:1 weight ratio. Total solids are 53 mg/ml.

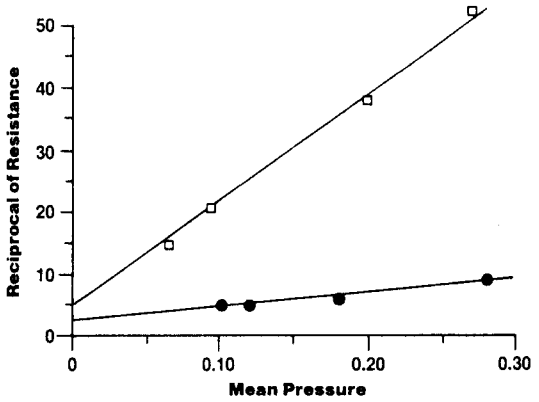

Figure 4—Reciprocal of closure resistance: pressure dependence. □, 20-mm closure; ●, 13-mm closure.

TABLE II Closure Mass Transfer Constants Defined by Eq. 18

Closure Size (mm)	$S0$	$S1$
13	2.3	22.4
20	4.8	169
28	8.1	406

pressure inside the tray is slightly higher than the chamber pressure, the stopper resistance, which is pressure dependent, is not identical for the two configurations. However, since the stopper resistance is small and the pressures are not greatly different, the approximation, $R_s = R_s'$, will suffice and nR_{tr} may be obtained by substraction of Eq. 15 from Eq. 16. The pressure in the tray, P_{tr}, may be obtained from,

$$\frac{nR_{tr}}{R_p + R_s + nR_{tr}} = (P_{tr} - P_c)/(P_0' - P_c). \qquad \text{(Eq. 17)}$$

The chamber resistance is evaluated from the chamber pressure, P_c, pressure in the condenser chamber P_{cd}, and the *total* sublimation rate (all vials), $N{\cdot}\dot{m}$, using Eq. 5.

"Representative Results"—Two types of closures of similar design were studied (19). The smaller closure is designed for use with vials of 13-mm OD neck, while the larger closure is used with vials of 20-mm OD neck. Both closures have two openings in the semi-stoppered position with effective circular diameter of 0.2 cm for the 13-mm size and 0.4 cm for the 20-mm size. The experimental data (Fig. 4) demonstrate that the reciprocal of closure resistance is a linear function of mean pressure, as expected (Eq. 6). Thus, there are two stopper mass transfer constants, denoted $S0$ and $S1$, defined by,

$$R_s^{-1} = S0 + S1\,\overline{P}, \qquad \text{(Eq. 18)}$$

where the constants are determined by regression analysis of the data (Fig. 4). The constants may also be calculated from the dimensions of the closure openings with useful accuracy (19). Experimental values of S0 and S1 are tabulated (Table II) for the 13-mm and 20-mm stoppers while estimated constants are given for 28-mm stoppers of the same basic design. The estimated constants were evaluated assuming the ratio of the calculated constant to the "experimental" constant is the same for the 28-mm stopper as observed for the 20-mm stopper (19).

The tray resistance was determined at only one pressure for trays of about 1500-cm² area equipped with a slightly elevated oversized lid which resulted in a vapor gap of about 1.5 cm along the circumference of the tray. The pressure dependence of the scaled tray resistance may be written,

$$(nR_{tr})^{-1} = T0 + T1{\cdot}\overline{P}. \qquad \text{(Eq. 19)}$$

For the lid design studied, the dimensions of the vapor gap are much larger than the mean-free path, and contributions from Knudsen flow should be negligible. Thus, $T0$ may be taken as zero. The value of $T1$, evaluated from the data, is 23. Note that the value of $T1$ is comparable in magnitude to the corresponding constant ($S1$) for 13-mm stoppers (Table II) indicating that the tray lid imposes a mass transfer barrier roughly equal to that imposed by a 13-mm stopper.

For the laboratory dryer, the reciprocal of the scaled chamber resistance, $(NR_c)^{-1}$, is also a linear function of mean pressure (19),

$$(NR_c)^{-1} = 4.6 + 71\overline{P}, \qquad \text{(Eq. 20)}$$

while preliminary data (21) indicate the scaled condenser resistance, NR_{cd}, is directly proportional to the partial pressure of inert gas (air) in the condenser chamber, P_2^{cd},

$$NR_{cd} = 0.055P_2^{cd}. \qquad \text{(Eq. 21)}$$

1.2 Heat Transfer Coefficients

1.21 Temperature Profile in Primary Drying: A temperature profile measured during primary drying in a pilot dryer (19) is illustrated by Figure 5. In this experiment, the vials were placed in an aluminum tray with a flat 5-mm thick bottom and a tray lid containing open channels for vapor flow (larger channels than for the lid design discussed in the previous section).

Heat transfer may be described in terms of four barriers or resistances to heat flow: (*1*) the shelf itself, with a temperature difference of 8 °C between the shelf interior and shelf surface; (*2*) the pan or tray, with a temperature dif-

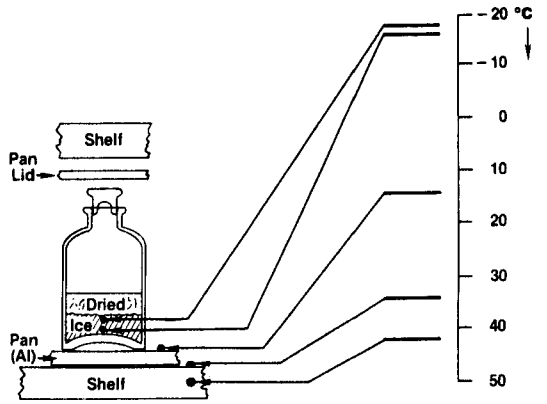

Figure 5—Temperature profile in primary drying: DOBUTREX (10 ml) in 5304 molded vials (8.3 cm²) in an aluminum tray; heat flux = 42 cal cm^{-2} hr^{-1}; chamber pressure 0.1 mmHg.

ference of 20 °C between the shelf surface and the top surface of the tray bottom; (3) the vial, with a temperature difference of 30° between the pan surface and the product in the bottom of the vial; and (4) the frozen product, with a temperature difference of about 2 °C between the ice at the vial bottom and the ice at the sublimation interface. The *thermal* resistance of a barrier may be defined as the ratio of the temperature difference across the barrier and the area normalized heat flow (18). Thus, the largest thermal resistance (50% of the total) is the vial/tray interface, but both the tray/shelf interface and the shelf itself contribute significantly to the total resistance, 33.3% and 13.3%, respectively. As defined here, the thermal resistance of the vial includes the thermal resistance of the glass in the vial bottom. Likewise, the tray resistance includes the thermal resistance of the aluminum in the tray bottom. However, the thermal resistance of the metal in an aluminum tray bottom is essentially zero (18), and the thermal resistance of the glass in the bottom of a vial is small (18, 19). Consequently, the thermal resistances of both the tray and the vial are due almost entirely to the vapor boundary existing between two solid surfaces not in perfect contact.

1.22 Definition of Heat Transfer Coefficients: A heat transfer coefficient is defined as the ratio of the area normalized heat flow, in cal s^{-1} cm^{-2}, to the temperature difference between heat source and heat sink. The shelf heat transfer coefficient, K_s, is defined in terms of the rate of heat flow, $\dot{Q}$, the shelf area per vial, ASV, and the temperature difference between the shelf interior (fluid temperature), T_f, and the shelf surface, T_s,

$$\dot{Q} = ASV\,K_s(T_f - T_s). \qquad \text{(Eq. 22)}$$

The thermal resistance, represented by the reciprocal of K_s, probably represents a combination of limited fluid flow through the shelf interior and a finite thermal conductivity of the shelf material itself. Thus, the shelf heat transfer coefficient is expected to be independent of chamber pressure and is likely quite sensitive to dryer design. Likewise, the tray heat transfer coefficient, K_{tr}, is defined by,

$$\dot{Q} = ATV\,K_{tr}(T_s - T_t), \qquad \text{(Eq. 23)}$$

where ATV is the tray area per vial and T_t is the surface temperature of the tray bottom. The vial heat transfer coefficient, K_v, is defined by,

$$\dot{Q} = A_v K_v(T_t - T_b), \qquad \text{(Eq. 24)}$$

where A_v is the cross-sectional area of the vial, calculated from the outer diameter of the vial, and T_b is the temperature of the product at the bottom center of the vial.

Since most of the heat input flows from the bottom of the vial to the subliming ice, the temperature of the product decreases as the distance from the bottom of the vial, X, increases. The usual proportionality between heat flow and temperature gradient is used (19) to define the effective thermal conductivity of the product, K_I,

$$\dot{Q}_B = -A_v K_I \frac{dT}{dX}, \qquad \text{(Eq. 25)}$$

where $\dot{Q}_B$ is the heat flow through the bottom of the vial and T is the temperature of the frozen product in the vial. Since the total area available for heat transfer, A_v, is in part glass but mostly frozen solution, one would expect K_I to be slightly smaller than the thermal conductivity of ice.

1.23 Measurement of Heat Transfer Coefficients: "Procedures"—Both the shelf heat transfer coefficient and the tray heat transfer coefficient are evaluated from the experiment described by Figure 5 and additional experiments of the same type. The heat transfer rate, $\dot{Q}$, is calculated assuming steady state,

$$\dot{Q} = \Delta\overline{H}s\,\dot{m}, \qquad \text{(Eq. 26)}$$

where $\Delta\overline{H}s$ is the heat of sublimation of ice (660 cal g^{-1}) (19), and $\dot{m}$ is the mean sublimation rate during the experiment, evaluated from the mass loss and the time of sublimation. The temperatures are directly measured (19).

Vial heat transfer coefficients were extensively studied using two slightly different procedures (19). The procedure giving the most accurate results for the mean K_v of a set of nominally equivalent vials, as well as the standard deviation in K_v for that set of vials, is termed the multivial experiment. Here, all vials investigated are filled with pure water to a depth of about 2 cm and each vial is weighed. To insure uniformity of mass transfer resistance, small precision bore stainless steel tubes of fixed length are inserted into each stopper, and the stopper is inserted fully into the vial neck. After loading and freezing, the shelf temperature and product temperature are adjusted to the expected steady-state sublimation temperature for that experiment, the chamber is quickly evacuated to the desired chamber pressure, and the shelf temperature is quickly increased to +5 °C. The entire experiment is conducted under conditions of constant shelf temperature and constant chamber pressure. After a time estimated to sublime about 2 g of ice, the dryer is vented, and each vial is weighed to obtain the mass loss for each vial. The average sublimation rate for each vial is calculated as the mass loss divided by the time of sublimation, and the total heat transfer rate is evaluated from Eq. 26. The vials are placed directly on the dryer shelf, and the temperatures, T_b and T_s, are directly measured (19). Normally, experiments at three or four chamber pressures between 0.05 mmHg and 0.4 mmHg are conducted for each type of vial studied. In principle, K_v is evaluated from the sublimation rate and temperature data by Eq. 24. However, while Eq. 24 assumes the temperature of the surface above the vials is the same as the shelf temperature, this condition is not met by the laboratory freeze dryer. Also, while the mean sublimation rate for all vials is directly measured, the product temperature is measured for only a few vials. Thus, in practice, the calculations are more complex (19). The relative standard deviation in K_v, for a set of nominally identical vials, is obtained from the standard deviation in sublimation rate, after contributions to the variance in sublimation rate arising from causes other than intervial variability in K_v are subtracted (19).

The effective product thermal conductivity, K_I, is determined by direct measurement of the product temperature as a function of the distance from the vial bottom. The heat transfer rate from the vial bottom (Eq. 25) is obtained by subtracting the contribution of radiative heat transfer to

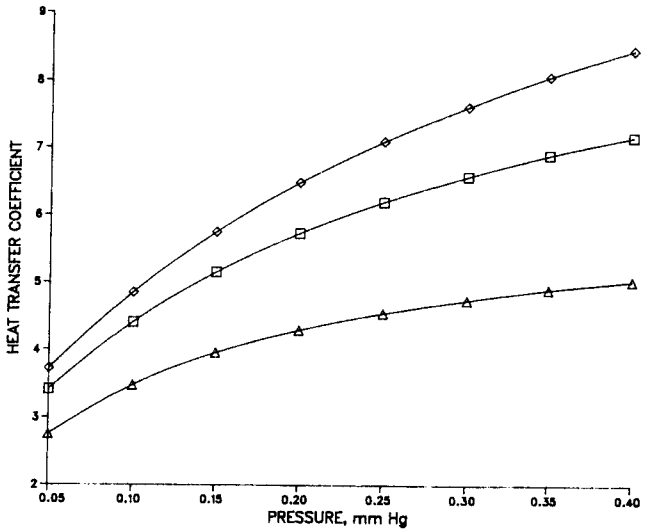

Figure 6—Pressure dependence of vial heat transfer coefficients for selected vials. □, W5816; ◇, K5816; △, 5303.

the top of the vial from the total heat transfer rate (19). Product temperature is a linear function of distance, and the value of K_f is determined by regression analysis of a plot of $\dot{Q}_B/A_v$ as a function of dT/dx.

"Representative Results"—Vial heat transfer coefficients increase with increasing pressure and depend strongly on the type of vial (Fig. 6). The data shown are smoothed experimental values for vials placed directly on a polished stainless steel shelf (19). The vial heat transfer coefficient is the sum of three contributions (19),

$$K_v = K_c + K_r + K_g, \qquad \text{(Eq. 27)}$$

where K_c is the contribution resulting from direct conduction from shelf to glass at the points of contact, K_r is the contribution from radiative heat transfer, and K_g is the contribution from conduction through the gas between the shelf and the vial bottom. Both K_c and K_r are independent of pressure, but K_g increases with increasing gas pressure according to the relationship,

$$K_g = \frac{\alpha \Lambda_0 P}{1 + l_v(\alpha\Lambda_0/\lambda_0)P}, \qquad \text{(Eq. 28)}$$

where Λ_0 is the free molecular heat conductivity of the gas at 0 °C; λ_0 is the thermal conductivity of the gas at ambient pressure, P is the gas pressure, and α is a function of the energy accommodation coefficient, a_c, and the absolute temperature of the gas, T,

$$\alpha = \frac{a_c}{2 - a_c}\sqrt{\frac{273.2}{T}}. \qquad \text{(Eq. 29)}$$

The parameter, l_v, represents the mean separation distance between the vial bottom and the surface upon which the vial rests (i.e., the shelf). Since data are available for λ_0 (26) and Λ_0 (17), Eq. 28 contains two parameters, the accommodation coefficient, a_c, and the separation distance, l_v, which must be evaluated from vial heat transfer data. Since the gas in the freeze drying chamber is nearly pure water vapor (19), Λ_0 and λ_0 refer to water vapor, and the accommodation coefficient is a measure of the efficiency of energy transfer in a collision between a water molecule and the surfaces involved (i.e., glass and shelf). While it may be assumed that the accommodation coefficient is independent of vial type, the value of l_v is obviously sensitive to the bottom geometry of the vial. Analysis of data for six different vial types yields, $a_c = 0.67$ (19).

The radiation contribution is a sum of two contributions, radiative heat transfer to the vial bottom and radiative heat transfer to the top of the vial from the surface above the vials. As a good approximation, the total radiative heat transfer coefficient may be expressed in the form,

$$K_r = 1.0{\cdot}10^{-4}(e_v + e_s), \qquad \text{(Eq. 30)}$$

where e_v is the effective emissivity for top radiation, and e_s is the emissivity of the surface upon which the vials are placed. In a series of experiments designed to independently evaluate e_v, it is found that e_v is 0.84 for all vials and products studied (19). The value of e_s is specific to the surface studied and may be directly measured using an optical pyrometer (19).

The pressure dependence of the vial heat transfer coefficient may be expressed in an alternate form equivalent to Eqs. 27 and 28,

$$K_v = KC + \frac{KP{\cdot}P}{1 + KD{\cdot}P}, \qquad \text{(Eq. 31)}$$

where KC is the sum of the contact parameter, K_c, and the radiative term, K_r, KP is the product, $\alpha\Lambda_0$, and KD is the combination of terms, $l_v(\alpha\Lambda_0/\lambda_0)$. With P in mmHg and K_v in cal s^{-1} cm^{-2} $°C^{-1}$, KP is $3.32{\cdot}10^{-3}$ for all vials. Values of KC and KD are specific to the vial (Table III). The values of KC were calculated using 0.56 for the emissivity, e_s, a value typical of steel (27). Contact parameter, K_c, and separation distance, l_v, data are taken from experimental studies (19) for the first four entries in Table III. The corresponding parameters for the 5305 vials are estimated from the geometry of the vial bottom using previously established correlations (19).

Tray heat transfer studies are much less extensive than the corresponding vial studies, and data are available only

TABLE III Vial Heat Transfer Parameters

Vial #	Type	Neck Finish (mm)	A_v (cm^2)	A_p (cm^2)	10^4 KC	KD
5800W	Tubing	20	4.71	3.80	2.64	3.64
5816W	Tubing	20	6.83	5.72	2.03	3.97
5304	Molded	13	8.30	6.07	1.82	5.18
5303	Molded	20	17.2	14.3	1.52	6.97
5305	Molded	28	20.8	17.6	1.52	8.05

TABLE IV Tray Heat Transfer Parameters Calculated with Accommodation Coefficient of Unity

Tray Type	$10^4\ K_{TR}$ ($P = 0.1$)	$10^4\ KTC$	KTD
Flat-bottomed aluminum	5.8	0.8	3.1
Warped stainless steel (mean of tray)	3.3	0.6	14.4
Warped stainless steel (area of maximum warp, 4 mm)	2.4	0.6	27

at one pressure, 0.10 mmHg (19). However, the heat transfer mechanisms should be formally the same as for the vial case and we write,

$$K_{tr} = KTC + \frac{KTP \cdot P}{1 + KTD \cdot P}, \qquad \text{(Eq. 32)}$$

where, as with the corresponding terms in the vial equation (Eq. 31), KTC is the sum of radiative and contact terms, KTP is "$\Lambda_0\alpha$" for the tray, and KTD is $l_T(\alpha\Lambda_0/\lambda_0)$, with l_T representing the mean separation distance between the tray bottom and the shelf surface. Since K_{tr} data are available at only one pressure (0.1 mmHg), two of the three parameters in Eq. 32 must be estimated. As a first approximation, we assume the accommodation coefficient is unity giving, $KTP = 6.59 \cdot 10^{-3}$. For the "flat" bottom aluminum tray, the mean separation distance is directly measured (0.02 cm), and KTD is then calculated. The constant term, KTC is then evaluated from K_{tr} at 0.1 mmHg. Since an average l_T for the warped stainless steel tray is difficult to determine by direct measurement, and the calculations are quite sensitive to the precise value of l_T chosen, an alternate procedure is used. Here, we assume negligible direct contact and further assume a radiative contribution only from the shelf to the tray bottom, giving $KTC = 0.6 \cdot 10^{-4}$. The value of KTD is then evaluated from the measured value of K_{tr}. The parameters obtained, as well as the experimental K_{tr} data at 0.1 mmHg, are listed in Table IV. Two sets of parameters are given for the warped tray since there is considerable variation in tray temperature with relative distance from an area of maximum warp.

The value of the shelf heat transfer coefficient, K_s, appears to be quite dryer specific. A value of $1.5 \cdot 10^{-3}$ cal s^{-1} cm^{-2} °C^{-1} was obtained for a pilot dryer (19) and is the value used for the calculations in this report. The value of K_s for the laboratory dryer (19) is about $1.0 \cdot 10^{-2}$, while preliminary data for a Stokes production dryer give a value of about $3 \cdot 10^{-3}$.

The temperature distribution in the frozen product is adequately described by a constant temperature gradient in the vertical direction and a single value of K_I, $5.9 \cdot 10^{-3}$ cal s^{-1} cm^{-1} °C^{-1}, for all vials and products studied (19). Originally we had expected that a radial temperature gradient in the vial would exist, such that the temperature at the bottom edge of the vial, T_E, would be slightly greater than the temperature at the bottom center, T_b. Thus, a radial temperature distribution constant, K_R, is defined by, $T_E - T_b = (T_b - T)(K_R - 1)$. However, it is found (19) that within the uncertainty in temperature measurement (±0.5 °C), $T_E = T_b$, so $K_R = 1$. Evidently, a measurable radial temperature gradient does not exist.

2. A Pseudo Steady-State Theoretical Model

2.1 Definition of the Model

The model assumes steady-state heat and mass transfer at each value of dried product thickness selected for the calculations. Further, the vapor in the vial interior is assumed to be 100% water. With $X_1^v = 1$, Eqs. 1 and 2 may be rearranged to give,

$$\frac{\dot{m}}{P_0} = A_p \hat{R}_p^{-1}(1 - P_v P_0). \qquad \text{(Eq. 33)}$$

Thus, $\dot{m}/P_0$ is predicted to be linear in P_v/P_0, and as an air leak into the chamber increases P_v/P_0 toward unity, the sublimation rate approaches zero. Since the sublimation rate will obviously not be negative for $P_v/P_0 > 1$, Eq. 33 is only an approximation, valid when $X_1^v \approx 1$.

The range of validity of $X_1^v \approx 1$ and Eq. 33 was investigated in a series of sublimation experiments with aqueous potassium chloride. Here, silicone stopcock grease was placed on the vial bottoms so that the product temperature, and therefore P_0, would be relatively insensitive to changes in chamber pressure. The sublimation rate was determined by weight loss measurements as a function of P_v/P_0, and corresponding vapor composition measurements (X_1^v) were made using procedures previously described (19). Under the conditions of the experiments, the normalized product resistance calculated from the parameters in Table I is approximately constant and equal to 2.6 for all experiments.

The sublimation rates (Fig. 7) are not particularly precise, presumably due to variations in $\hat{R}_p$ caused by uncontrolled freezing variations [5% KCl appears particularly notorious in this regard (4)]. However, the sublimation rate data are consistent with Eq. 33 until the ratio P_v/P_0 reaches about 0.8–0.9. For values of P_v/P_0 exceeding unity, the sublimation rates are very small but are clearly not zero. Similarity, X_1^v is essentially unity until P_v/P_0 is in the range 0.8–0.9. Thus, it appears that the assumption $X_1^v = 1$ restricts the theoretical model to values of P_v/P_0 less than about 0.8. It should be noted that for P_v/P_0 ratios in this

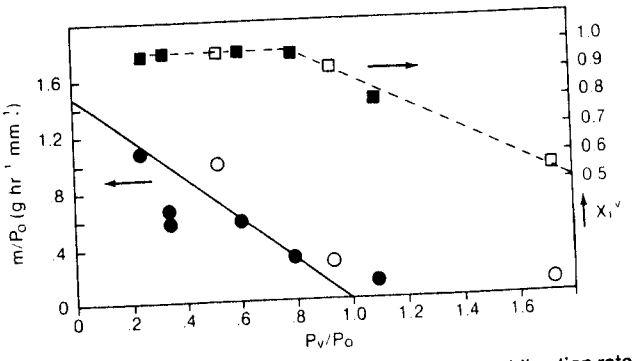

Figure 7—Effect of increasing chamber pressure on sublimation rate at constant product temperature: 5% (v/v) KCl in 5800W vials; ●, $\dot{m}/P_0$ at −23°; ○, $\dot{m}/P_0$ at −30°; —, $\dot{m}/P_0$ from Eq. 33 with mean $\hat{R}_p$ of 2.6; ■ X_1^v at −23°; □ X_1^v at −30°; - - - - - - - smoothed curve for X_1^v.

range, $P_v \cong P_c$, so an equivalent restriction is, $P_c/P_0 \leq 0.8$.

From the defining equations for heat and mass transfer coefficients given in preceeding sections of this report, a set of six equations describing heat and mass transfer in primary drying are developed,

$$G1 = (\hat{R}_p/A_p + R_s + nR_{tr})\cdot\dot{m} - P_0 + P_c = 0, \quad \text{(Eq. 34)}$$

$$G2 = R_s\dot{m} - P_v + P_{tr} = 0, \quad \text{(Eq. 35)}$$

$$G3 = nR_{tr}\cdot\dot{m} - P_{tr} + P_c = 0, \quad \text{(Eq. 36)}$$

$$G4 = 0.1833\ \dot{m}[(A_v\cdot K_v)^{-1} + (ATV\cdot K_{tr})^{-1} + (l_m - l) \times (A_pK_I)^{-1}] - T_s + T = 0, \quad \text{(eq. 37)}$$

$$G5 = 0.1833\ \dot{m}(A_vK_v)^{-1} - T_t + T_b = 0, \quad \text{(Eq. 38)}$$

$$G6 = 0.1833\ \dot{m}(ATV\cdot K_{tr})^{-1} - T_s + T_t = 0. \quad \text{(Eq. 39)}$$

The numerical term, 0.1833, is a result of the relationship between sublimation rate, $\dot{m}$, in ghr^{-1} and the heat flow rate, $\dot{Q}$, in cal s^{-1} (Eq. 26). The term, l_m, is the thickness of the frozen product at time zero calculated from

$$l_m = \frac{V}{\rho_I A_p}, \quad \text{(Eq. 40)}$$

where ρ_I is the density of ice and V is the fill volume. Thus, $l_m - l$, is the thickness of the ice in the vial for any given value of dried product thickness, l. Note that the thermal resistance of the frozen product included in Eq. 37 (i.e., the term in K_I) is an approximation which assumes $\dot{Q}_B \approx \dot{Q}$ (Eq. 25). The error introduced by this approximation is not significant.

Many of the "variables" in Eqs. 34–39 are functions of other variables. The vapor pressure of ice, P_0, is related to sublimation temperature, T (4),

$$P_0 = 2.6983\cdot 10^{10} \exp(-6144.96/T), \quad \text{(Eq. 41)}$$

the normalized product resistance is related to temperature and dried product resistance by Eq. 12, while R_s and nR_{tr} are functions of pressure (Eqs. 18 and 19). Similarly, the heat transfer coefficients, K_v and K_{tr}, are functions of pressure through Eqs. 31 and 32. Thus, for a fixed value of dried product thickness, l, the functions, G1 through G6, define a set of six equations in eight variables: $\dot{m}$, T, T_b, T_t, T_s, P_v, P_{tr}, and P_c. Once two of the variables are fixed, for example the chamber pressure, P_c, and the shelf surface temperature, T_s, the six equations may be solved simultaneously to obtain the other six variables.

2.2 *Method of Solution*

The calculation procedure, illustrated by Table V, involves dividing primary drying into five stages by appropriate choices of the dried product thickness, l, where

$$l = n\, l_m/5. \quad \text{(Eq. 42)}$$

Here, n is an integer ranging from 0 to 5, and l_m is the maximum thickness of the dried product layer (i.e., l at the end of primary drying) given by Eq. 40. In each stage, the ice-vapor boundary recedes a fixed distance, $l_m/5$. In the example shown (Table V), l_m is 1.0 cm and each stage corresponds to a 0.2-cm movement of the boundary. In this example, the shelf surface temperature, T_s, and the chamber pressure, P_c, are fixed at constant values throughout each stage, but are allowed to be different for the different stages of drying. For each stage, a computer-assisted solution of Eqs. 34–39 is obtained for the l value at the start of that stage and also for the l value at the end of that stage. For example, for Stage 1, computer solution #1 yields parameters for $l = 0$, while computer solution #2 yields parameters for $l = 0.2$ cm, both solutions being obtained for shelf temperature T_1 and chamber pressure P_1. The resulting sublimation rates, $\dot{m}(1)$ and $\dot{m}(2)$, are then used to evaluate the mean sublimation rate over the l interval of $0 \leq l \leq 0.2$ cm. as the simple mean of $\dot{m}(1)$ and $\dot{m}(2)$. The time interval required to complete the jth stage, Δt_j, is evaluated from the mass of ice sublimed in a given stage, Δm, and the mean sublimation rate for that stage, $\langle \dot{m}_j \rangle$,

$$\Delta t_j = \frac{\Delta m}{\langle \dot{m}_j \rangle} = \frac{\rho_I \Delta l A_p \epsilon}{\langle \dot{m}_j \rangle}, \quad \text{(Eq. 43)}$$

where ϵ is the volume fraction of ice in the frozen system and Δl is the boundary movement during completion of one stage, 0.2 cm for the example shown (Table V). The accumulated drying time corresponding to a given value of l is then given by,

$$t_i = \sum_{j=1}^{i} \Delta t_j, \quad \text{(Eq. 44)}$$

where t_i is the total time expired at the end of the ith drying

TABLE V Method of Solution and Introduction of Time Dependence: Example for l_m = 1.0 cm: Process variables T_s, P_c Fixed

Drying Stage #	Computer Solution #	l	T_s	P_c	$\dot{m}$	Δt
1	1	0	T_1	P_1	$\dot{m}(1)$	
	2	0.2	T_1	P_1	$\dot{m}(2)$	Δt_1
2	3	0.2	T_2	P_2	$\dot{m}(3)$	
	4	0.4	T_2	P_2	$\dot{m}(4)$	Δt_2
3	5	0.4	T_3	P_3	$\dot{m}(5)$	
	6	0.6	T_3	P_3	$\dot{m}(6)$	Δt_3
4	7	0.6	T_4	P_4	$\dot{m}(7)$	
	8	0.8	T_4	P_4	$\dot{m}(8)$	Δt_4
5	9	0.8	T_5	P_5	$\dot{m}(9)$	
	10	1.0	T_5	P_5	$\dot{m}(10)$	Δt_5

stage. Thus, the time dependence of l is established, and the total primary drying time is given by Eq. 44 with $i = 5$.

The computer program required to solve the transport equations and tabulate the results is written in MLAB. MLAB is a general purpose model fitting computer program package available from the Division of Computer Research and Technology at the National Institute of Health, Bethesda, Md. A listing of the program is given in the *Appendix*. A "fit" statement in MLAB is used to solve the set of equations. In essence, the computer adjusts, by an iterative procedure, the unknown parameters to minimize the squares of the functions G1 through G6. When further adjustment in parameters fails to reduce the magnitude of the G functions, "convergence" is obtained, and the "best fit" parameters are printed. As a check on the accuracy of the resulting solution, the residual sum, $(G1^2 + G2^2 + \ldots + G6^2)^{1/2}$, is also calculated. Generally, the residual is on the order of 10^{-6}, and the parameters obtained from the solution are accurate to roughly the same order of magnitude.

Use of the program proceeds by the following sequence:

1. The desired shelf temperatures in °C are input in the form of a 5×1 matrix denoted ST by, ST__LIST (t_1, $t_2, \ldots, t_5$).
2. The desired chamber pressures in mmHg are input in the form of a 5×1 matrix denoted PS by, PS__LIST ($P_1, P_2, \ldots, P_5$).
3. The tray mass and heat transfer parameters (Eqs. 19 and 32) are input as scalars. For vials placed directly on the shelf, *KTC*, and *KTP* are set equal to a large number (100) and *KTD* is set at unity. If no tray lid is used, $T1$ is set at a very large number (1×10^6).
4. The vial heat and mass transfer parameters and geometric parameters for each vial type are stored in separate data files. The parameters corresponding to the vials of interest are input by calling the appropriate file by a command of the form, DO V5800W, where V5800W is the data file for 5800W type vials.
5. The dried product resistance parameters (Eq. 12) are stored in separate data files for each product. Data for the product of interest are input by a command of the form, DO PVP5.
6. The fill volume in ml desired is input as a scalar, i.e., V__5, sets the fill volume at 5 ml.
7. The volume fraction of ice in the frozen product, E, is input as a scalar, i.e., E__.9.
8. The functions G1 through G6 and the auxiliary functions [i.e., $P_0(T)$, $\hat{R}_p(l), \ldots$] are defined by calling a data file defining all the functions. The command, DO FDFN, is used.
9. The program is run by the command, DO FDRY.

Output of the program is a series of tables and plots giving the total drying time as well as:

1. All mass transfer resistances (R_p, R_s, R_{tr}) as a function of l;
2. All pressures (P_0, P_v, P_{tr}, P_c) as a function of time;
3. All temperatures (shelf, tray, vial at bottom edge, vial at bottom center, and subliming ice) as a function of time;
4. The sublimation rate and the residual sum of the fit for each computer solution of the equation set.

The above discussion refers to the program version where the shelf temperature and chamber pressure are fixed for each stage of drying. An alternate version of the program, where the sublimation temperature is fixed throughout the cycle, is available. Here, the sublimation temperature, T, is input as a scalar in °K, an alternate function file is input by, DO FDFNT, and the program is run by the command, DO FDRYT. The rest of the operating sequence is the same as outlined above except the shelf temperatures are not input data but rather are parameters determined by the computer solution of the equation set. The output data is essentially the same as summarized above.

The actual computer time required to run either version of the program is minimal (~10 sec), but since we run the program on a time-sharing system, the total time required is much longer (~10 min).

2.4 *Comparison of Theory and Experiment*

A series of freeze drying experiments using the pilot-scale dryer (19) were carried out to check the accuracy of the "computer simulated" freeze-drying results. Each experiment represents one run at constant chamber pressure and constant shelf interior (fluid) temperature. The shelf temperature/time profile during freezing was the same for all experiments: 0 °C (30 min)/−25 °C (60 min)/−40 °C (until all product < −30). The computer calculations used the input data presented in this report. The shelf of the pilot dryer has an emissivity of 0.95 (19) instead of the 0.56 value used in the calculations. However, the surface above the vials also runs somewhat colder than the shelf surface so the total radiative contribution to K_v assumed by the theory is a good approximation.

Although the theoretical model does not explicitly contain the shelf heat transfer coefficient, calculations involving shelf heat transfer and the resulting temperature differences between shelf fluid and shelf surface may be carried out when the vials are directly on the shelf. One may simply use the tray heat transfer equations to represent shelf heat transfer. Thus, *KTC* is set equal to K_s while *KTP* is set at zero. The shelf temperature, T_s, in the program becomes the shelf interior temperature, T_f, and the tray temperature, T_t, becomes the shelf surface temperature, T_s.

The results of the comparison (Table VI) demonstrate that the theoretical calculations are quantitative, the agreement in cycle times being particularly impressive. The cycle time is the total primary drying time. The experimental cycle time is taken as the time corresponding to the inflexion point in the product temperature vs. time curve, which occurs shortly after the product temperature begins to increase sharply. The maximum product temperature is the temperature of the product just before the sharp increase in product temperature near the end of primary drying. Experimentally, this parameter is difficult to determine accurately and is probably accurate only within ±2 °C. The mean product temperature is the average product temperature throughout primary drying at the bottom center of the vial.

TABLE VI Comparison of Theory with Experiment: Pilot Dryer with Vials Directly on the Shelf with No Tray Lid

Product	Vial	Fill Volume (ml)	Shelf Interior °C	P_c (mm)	Cycle Time (hr)	Temperature, °C Shelf Surface	Mean Product	Maximum Product
PVP (5%)	W5816	8	−5	0.10	25.8[a]	−9.6[a]	−27.8[a]	−25.3[a]
					26.9[b]	−9.9[b]	−27.3[b]	−24.6[b]
Mannitol (5%)	W5816	8	−5	0.10	33.4[a]	−8.6[a]	−22.4[a]	−20.2[a]
					34.8[b]	−8.9[b]	−22.9[b]	−18.5[b]
Mannitol (5%)	W5816	8	+15	0.10	19.2[a]	+6.2[a]	−17.0[a]	−14.2[a]
					19.1[b]	+8.0[b]	−17.0[b]	−11.8[b]
Mannitol (5%)	W5816	8	+15	0.40	14.0[a]	+5.7[a]	−13.0[a]	−11.9[a]
					15.8[b]	+6.6[b]	−11.8[b]	−8.0[b]
Mannitol (5%)	5303	20	+15	0.40	19.2[a]	+6.1[a]	−14.5[a]	−12.8[a]
					19.0[b]	+8.1[b]	−13.5[b]	−9.7[b]

[a] Experimental.
[b] Theoretical.

3. Applications of the Theoretical Model

3.1 Effect of the Product Temperature on Drying Time

The effect of product temperature (sublimation temperature) is investigated by using the FDRYT version of the program where the sublimation temperature, T, is fixed at selected values for the series of calculations. Representative results (Fig. 8) indicate that, in general, the drying time is roughly linear in sublimation temperature on a semi-log plot where the drying time decreases by about 13% for a 1 °C increase in temperature. The deviation in linearity at higher temperatures shown by DOBUTREX is a result of the temperature dependence in $\hat{R}_p$ for DOBUTREX. The product resistance for DOBUTREX decreases sharply as the temperature increases above −20 °C. Clearly, the efficiency of primary drying is strongly temperature dependent, and therefore, the heat input during primary drying should be adjusted to yield a sublimation temperature as close to the collapse (or eutectic) temperature as possible. Clearly, uncertainty in temperature measurement and intervial variability in sublimation temperature demand a "safety" margin, but this safety margin should be minimized for efficient operation.

3.2 Effect of Process Variables: Shelf Temperature and Chamber Pressure

Both the response of the product temperature to shelf temperature changes as well as the product temperature at any given shelf temperature are quite dependent on details of the freeze drying conditions (Fig. 9). The increase in product temperature resulting from a 10 °C increase in shelf surface temperature varies from slightly less than 2 °C to slightly more than 6 °C for the conditions studied (Fig. 9). The drying time at fixed shelf temperature is also quite specific to conditions (Fig. 10). In the examples shown (Figs. 9 and 10), a constant fill volume was used. Thus, the product freeze dried in the larger 5303 vials exhibited a much smaller product resistance due to larger product area and smaller maximum dried product thickness. At least for mannitol, the lower resistance dominates the freeze-drying behavior. Thus, in spite of a lower heat transfer coefficient for the 5303 vials, sublimation is faster in the 5303 vials

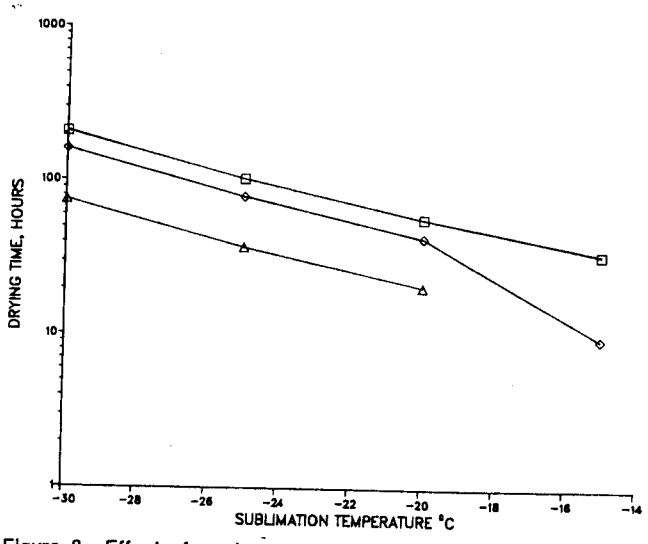

Figure 8—Effect of product temperature on drying time: chamber pressure 0.1 mmHg; 5800W vials; 8 ml fill volume: □, 5% mannitol; ◇, DOBUTREX; △, 5% *PVP*.

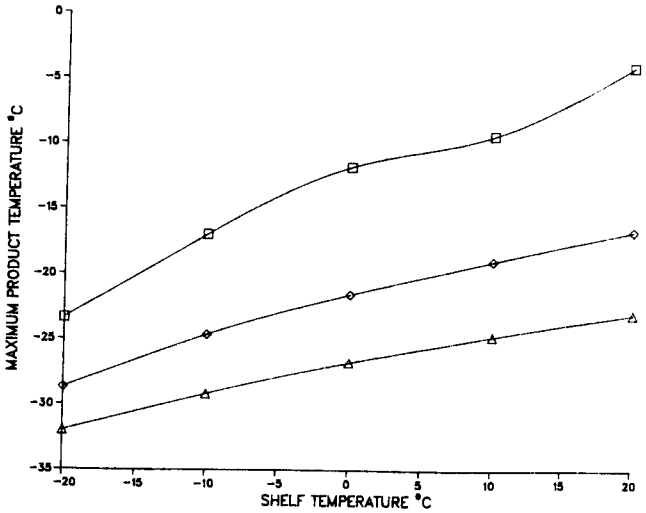

Figure 9—Effect of shelf temperature on maximum product temperature of 5% (w/w) mannitol: P_c = 0.10 mmHg; fill volume, 8 ml: □, 5800W; ◇, 5303; △, 5303 (maximum warp tray).

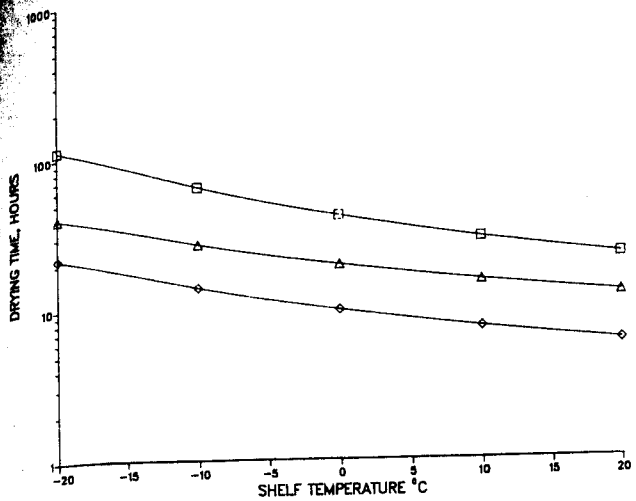

Figure 10—Effect of shelf temperature on drying time of 5% (w/w) mannitol: P_c = 0.10 mmHg; fill volume, 8 ml: □, 5800W; ◊, 5303; △, 5303 (maximum warp tray).

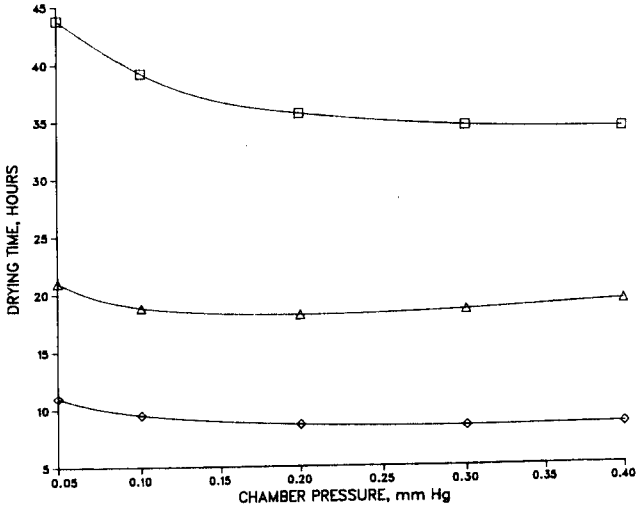

Figure 11—Effect of chamber pressure on drying time of 5% (w/w) mannitol; shelf temperature, 0 °C; fill volume, 8 ml: □, 5800W; ◊, 5303; △, 5303 (maximum warp tray).

than in the 5800W vials (Fig. 10), and the product temperature is lower (Fig. 9). The effect of an additional thermal barrier is clearly demonstrated by comparing the results (Figs. 9 and 10) for 5303 vials directly on the shelf (diamonds) with the corresponding results for 5303 vials near an area of maximum warp in a stainless steel pan with no lid (triangles). The additional thermal barrier imposed by the warped tray bottom results in both a lower product temperature and a longer drying time (factor of 2) than found for vials placed directly on the shelf. To obtain the same freeze-drying behavior for vials in a warped pan as for vials placed directly on a −10 °C shelf, the shelf surface needs to be about +20 °C.

Since both the vial heat transfer coefficient and the tray heat transfer coefficient increase with increasing pressure, more heat is supplied to the sample as the chamber pressure is increased at fixed shelf temperature. Thus, the drying time normally decreases as the chamber pressure increases (18). However, the driving force for mass transfer from the ice-vapor interface to the chamber is the pressure difference, $P_0 - P_c$, and while an increase in P_c usually increases the product temperature sufficiently to produce an increase in $P_0 - P_c$, thereby increasing the driving force, there are circumstances where an increase in chamber pressure decreases the driving force. Theoretical results giving the effect of chamber pressure on drying time (Fig. 11) and maximum product temperature (Fig. 12) for a 0 °C shelf show the expected decrease in drying time and increase in product temperature as the pressure increases from low values. However, at higher pressures, the drying time passes through a shallow minimum as pressure increases (Fig. 11). The corresponding product temperatures (Fig. 12) increase with increasing pressure at all pressures, although the sensitivity to pressure decreases at higher pressure. The position of the minimum in the drying time vs. pressure curve depends on the drying conditions. For the 5800W vials, the minimum is above 0.4 mmHg, but for 5303 vials in a warped tray, the minimum occurs around 0.2 mmHg. In general, this minimum will be at relatively low pressure when the total separation distance between vial bottom and shelf surface is large since under these conditions, heat transfer coefficients are less sensitive to pressure (Eqs. 31 and 32).

The heat input required to maintain a given product temperature may be controlled by either shelf temperature or chamber pressure adjustments. Thus, if the objective of the process design is to control the product temperature at a given value, one may choose either high shelf temperature and low chamber pressure or low shelf temperature and high chamber pressure. In general, the option involving low chamber pressure is preferred since, by this choice, the driving force is maximized, resulting in a shorter drying time. In practice, as long as the chamber pressure is small compared to the vapor pressure of ice at the product control temperature, any combination of shelf temperature and chamber pressure that produces the desired product temperature will give essentially the same drying rate.

3.3 Selection of the Optimum Container

Although selection of the container (vial) may well be

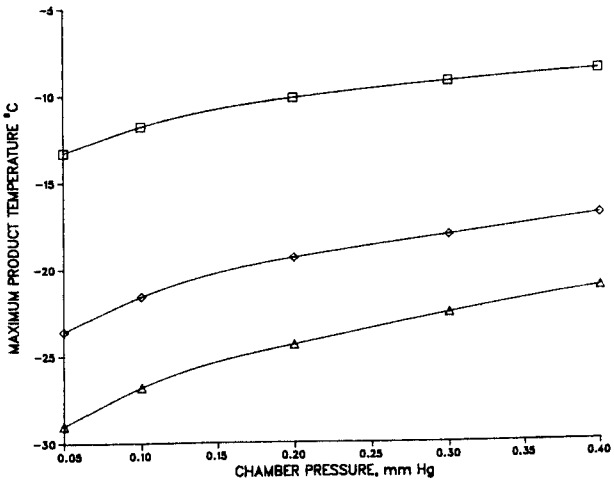

Figure 12—Effect of chamber pressure on maximum product temperature of 5% (w/w) mannitol; shelf temperature, 0 °C; fill volume, 8 ml: □, 5800W; ◊, 5303; △, 5303 (maximum warp tray).

dictated by considerations other than efficiency of the freeze-drying process, we assume here that the optimum container is the container which yields the greatest efficiency in freeze drying. The efficiency is defined as the number of vials produced per day per unit area of dryer shelf space. The total cycle time must be used to evaluate the rate of vial production, where the total cycle time is the sum of the freezing time, primary drying time, secondary drying time, and the time required for dryer preparation and loading. For purposes of this illustration, the sum of the freezing, secondary drying, and loading times is fixed (Table VII) at 10 hr for all vials. Variation in cycle time is then due to variation in primary drying time. For each product/vial combination, the sublimation temperature is fixed (at −20 °C) and the chamber pressure is fixed (at 0.10 mmHg), and the calculations are performed using the FDRYT version of the computer program. Since the dose is fixed, larger vials will have a larger product area, A_p, and a smaller value of maximum dried product thickness, l_m, both effects yielding a smaller dried product resistance and a corresponding shorter drying time. On the other hand, the number of vials per unit area of dryer shelf is smaller for the large vials. The number of vials per unit shelf area is computed from the vial area, A_v, assuming a 95% packing efficiency.

The calculated efficiency data (Table VII) indicate that, for both products considered, the efficiency is a maximum for the 5816W vials. The least efficient vial depends on the product, 5303 for PVP and 5800W for mannitol.

3.4 *Estimation of Process Nonuniformity*

The results discussed in previous sections of this report refer to the behavior of the average vial. In practice, due to numerous causes, an inter-vial distribution of product temperatures and drying times exist, and nonuniformity effects must be considered in process optimization. Given some experimental data, the theoretical model may be used to estimate nonuniformity effects. In the discussion which follows, vials are assumed to be directly on the dryer shelf.

The response of a dependent freeze-drying parameter, denoted Y (drying time or product temperature), to variation in an independent parameter, denoted X_i (source of process nonuniformity), is calculated from,

$$\sigma^2(Y) = \left(\frac{\partial Y}{\partial X_i}\right)^2_{T_F,P_c} \sigma^2(X_i), \qquad \text{(Eq. 45)}$$

where $\sigma^2(Y)$ is the variance introduced into the dependent parameter by the variance in the independent parameter $\sigma^2(X_i)$. Since we wish to evaluate, for example, the effect of variability in K_v *within the same freeze drying run*, the partial derivative refers to a rate of change evaluated at constant time average fluid temperature (T_F) and chamber pressure (P_c). The value of $\sigma^2(X_i)$ is evaluated from experimental data, for example, from the relative standard deviation in vial heat transfer coefficient, $\sigma(K_v)$. The theoretical model is used to calculate the partial derivative. First, the fluid temperature sequence that will produce the desired sublimation temperature throughout a run at a selected constant pressure is evaluated by using the FDRYT version of the program. Next, using this sequence, the FDRY program is run first with the X_i parameter at its mean value (i.e., usual value of K_v for that vial), and then with the X_i parameter incremented by one standard deviation. Since the standard deviations, $\sigma(X_i)$, are small, the derivative is approximated as $\Delta Y/\Delta X_i$, where ΔY is the calculated change in the dependent parameter of interest, and $\Delta X_i = \sigma(X_i)$. Since the computer calculations are based on a T_f sequence corresponding to fixed increments in l, not time, the time average T_f is not exactly the same for the two calculations. Thus, the constant T_f requirements of the partial derivative are not rigorously met. However, numerical calculations show that the error introduced is negligible.

The precise meaning of $\sigma(TD)$, where TD is drying time, requires further comment. As defined and calculated, $\sigma(TD)$ is the standard deviation in drying time where all vials are exposed to the same time average shelf interior temperature. Since TD is calculated as the ratio of total water content to time average sublimation rate, the *relative* standard deviation in TD is identical to the *relative* standard deviation in time average sublimation rate. Thus, a slow drying vial with its TD increased by 1% over the mean will have a 1% slower time average sublimation rate, and

TABLE VII. Selection of Optimum Container: 8 ml Fill Volume, −20 °C Sublimation Temperature, 0.10 mmHg Chamber Pressure

Total Cycle = Primary + 2 (freeze) + 6 (secondary) + 2 (load. .)

Vial #	A_r (cm²)	l_m (cm)	Primary Dry (hr)	Efficiency # Vials m^{-2} day^{-1}
		5% (v/v) PVP		
5800W	4.71	2.29	20.7	1581
5816W	6.83	1.52	10.3	1648
5304	8.3	1.44	10.7	1330
5303	17.2	0.61	2.46	1066
		5% (w/w) Mannitol		
5800W	4.71	2.29	57.1	723
5816W	6.83	1.52	26.6	914
5304	8.3	1.44	25.5	775
5303	17.2	0.61	5.19	875

therefore, at time TD, when the average vial is dry, the slow drying vial will have "residual ice" equivalent to 1% of the initial amount. If the drying process were continued at *the same time average sublimation rate*, the slow vial would take 1% longer to dry. However, since in general, the sublimation rate decreases as a function of time, the sublimation rate corresponding to removal of the "residual ice" is less than the average sublimation rate over the first TD hours of the process, and the extension in drying time is therefore more than 1%. The extension in drying time may be approximately evaluated by first evaluating the residual ice present in a slow drying vial, deviating from the mean by S standard deviations,

$$m_R = m_0 S \cdot \frac{\sigma(TD)}{TD}, \qquad \text{(Eq. 46)}$$

where m_R is the mass of residual ice, and m_0 is the initial mass of ice. Assuming the shelf fluid temperature and chamber pressure used in the last stage of primary drying are maintained, the time required to complete drying of this vial, denoted delay time, is calculated from the sublimation rate for an average vial at the end of its primary drying, $\dot{m}(l_m)$, available from the computer output,

$$\text{Delay Time} = \langle \dot{m} \rangle_t \, S\sigma(TD)/\dot{m}(l_m), \quad \text{(Eq. 47)}$$

where $\langle \dot{m} \rangle_t$ is the time average sublimation rate, m_0/TD.

"Effects of Nonuniformity in Shelf Temperature"—In general, one may expect that the shelf surface temperature in the dryer is not pefectly uniform during primary drying. A limited amount of data for a pilot dryer (19) indicates that temperature differences between different positions on the same shelf are directly proportional to the heat transfer rate, $\dot{Q}$, where the temperature distribution with position is a result of constant temperature gradients, with respect to distance, across the shelf "left to right" (x direction) and across the shelf "back to front" (y direction). We assume the shelf temperature distribution is a result of a corresponding distribution in shelf heat transfer coefficient, K_s (Eq. 22). Thus, the fluid temperature, T_f, is taken as a constant and differentiation of Eq. 22 yields,

$$\frac{dK_s}{K_s} = \frac{dT_s}{T_f - T_s}, \qquad \text{(Eq. 48)}$$

where dK_s is the differential change in K_s corresponding to the differential change in T_s, dT_s. Using Eq. 48, measured temperature differences may be translated into differences in K_s. The temperature data indicate roughly a 40% decrease in K_s from back to front (y direction) and a 24% increase in K_s from left to right (x direction). Assuming that the deviation in K_s from the mean value is bilinear in x and y, one may show that the above differences in K_s produce an effective relative standard deviation in K_s of about 13%. Since K_s is $1.5 \cdot 10^{-3}$ cal s^{-1} cm^{-2} $°C^{-1}$, the effective standard deviation in K_s, $\sigma(K_s)$, is then $\pm 2 \cdot 10^{-4}$ cal s^{-1} cm^{-2} $°C^{-1}$. Although $\sigma(K_s)$ is not based upon a normal distribution, it is assumed that this lack of statistical rigor may be ignored without serious consequence.

Calculations of the effect of shelf temperature variation are then carried out by comparing the theoretical results with K_s set at the average value with the corresponding results when K_s is set at the average value plus one standard deviation. For example, the resulting product temperature change is the standard deviation in product temperature arising from nonuniformity of shelf temperature. As indicated earlier, shelf heat transfer effects are calculated by using the tray heat transfer equations parameterized for shelf heat transfer. Calculations were performed using the FDRY program with the shelf interior temperature sequence selected to maintain the sublimation temperature at −25 °C when K_s is the average value. Calculated standard deviations in both sublimation temperature, t_{ice}, and drying time, TD, due to nonuniformity in shelf surface temperature, are given (Table VIII) for two vial types at several chamber pressures. As expected, the standard deviations in both drying time and sublimation temperature are slightly higher for the 5816W vials which have larger vial heat transfer coefficients. The significant increase in drying time as the chamber pressure, P_c, increases is a result of the decrease in driving force, $P_0 - P_c$, as P_c increases. The vapor pressure of ice, P_0, is constant since the mean drying times calculated all refer to a sublimation temperature of −25 °C.

"Effects of Nonuniformity in Vial Heat Transfer Coefficient"—The relative standard deviation in the vial heat transfer coefficient may be attributed to two sources of variation (19): variation in the pressure independent term in Eq. 31, represented by the relative standard deviation in KC, $\sigma(KC)$; and variation in the term including the separation distance, represented by the relative standard deviation in KD, $\sigma(KD)$. While these relative standard deviations do appear to vary with vial type (19), average values of $\sigma(KC) = 7.0\%$ and $\sigma(KD) = 8.9\%$ are used for the present calculations. The calculation procedure is analogous to the procedure used to evaluate effects of the variation in K_s. In separate calculations, the drying time change and product temperature change corresponding to one standard deviation change in both KC and KD are determined. The variance produced by KD variations and KC variations are assumed additive. Thus, for example, the standard deviation in product temperature arising from variability in K_v is

TABLE VIII. Effect of Nonuniform Shelf Surface Temperature: 5% Povidone; Sublimation Temperature −25 °C; l_m = 1.523 cm

Chamber Pressure (mmHg)	Drying Time TD (hr)	$\sigma(TD)$ (hr)	$\sigma(t_{ice})$ °C
	Vials 5816W (high K_v*)*		
0.05	19.411	0.316	0.139
0.10	21.197	0.406	0.143
0.20	28.158	0.630	0.120
0.30	42.889	1.039	0.086
	Vials 5305 (low K_v*)*		
0.05	19.828	0.276	0.119
0.10	21.514	0.348	0.122
0.20	28.349	0.522	0.103
0.30	43.680	0.853	0.069

TABLE IX. Effect of Nonuniform Vial Heat Transfer Coefficient: 5% Povidone; Sublimation Temperature, −25 °C; l_m = 1.523 cm

Chamber Pressure (mmHg)	$\sigma(TD)$ (hr)	$\sigma(t_{ice})$ °C
	Vials 5816W (high K_v)	
0.05	0.493	0.219
0.10	0.411	0.145
0.20	0.498	0.094
0.30	0.802	0.066
	Vials 5305 (low K_v)	
0.05	0.553	0.241
0.10	0.525	0.184
0.20	0.717	0.141
0.30	1.184	0.095

given by, $\sqrt{(\Delta t_1^2 + \Delta t_2^2)}$, where Δt_1 is the product temperature change caused by a variation of 7.0% in KC and Δt_2 is the temperature change caused by a variation of 8.9% in KD.

The calculated standard deviations arising from variability in vial heat transfer coefficient (Table IX) are similar in magnitude to the corresponding standard deviations resulting from variability in shelf surface temperature (Table VIII) and show the same qualitative trends with chamber pressure. Assuming the total variance in a property (square of standard deviation) is a sum of component variances (vial and shelf), the total variance in TD is calculated from the standard deviation data reported in Tables VIII and IX. The percentage of total variance attributable to K_v variations in the 5816W vials decreases from 71% at 0.05 mmHg to 37% at 0.3 mmHg; while the corresponding decrease for the 5305 vials is from 80% to 66%. Thus, at low pressure, the dominant cause of heat transfer variation is variation in vial heat transfer coefficient, at least for a freeze dryer with shelf temperature uniformity equivalent to, or better than, our pilot dryer.

"Effects of Improper Closure Position"—While the closure resistance is normally small compared to the dried product resistance, variation in position of the closure can be a factor in process variability. The area available for vapor flow from the vial interior is dependent upon how deep the stoppers are pushed into the vial neck in the "semi-stoppered" position. While production filling lines attempt to control this position, a small statistical variation certainly exists. More seriously, observations indicate that on occasion, a stopper is pushed into the vial neck far beyond the correct depth. The impact of such an improperly positioned closure on the freeze-drying behavior is explored in Table X. The first row (Table X) refers to freeze drying without a closure present and serves as the "base line" for the other calculations. The increase in product temperature near the end of primary drying and the percentage increase in drying time over the "no closure" configuration are listed for various closure positions. All calculations used a shelf temperature sequence which gives a −25° sublimation temperature for the "no closure" configuration. The calculations for 1/2-closed and 3/4-closed are based on closure mass transfer parameters, $S0$ and $S1$, being decreased by factors of 2 and 4, respectively, thereby increasing the closure resistances by the factors of 2 and 4.

TABLE X. Effect of Improper Closure Position: 5% Povidone; 8 ml Fill; K_v for 5816 Vials; Chamber Pressure 0.1 mmHg; Sublimation Temperature, −25 °C

Closure Position	Increase in $T(l_m)$, °C	% Increase in Drying Time
None	0	0
	20-mm Closure	
Normal	0.16	1.0
1/2-Closed	0.30	1.9
3/4-Closed	0.55	3.4
	13-mm Closure	
Normal	0.67	4.2
1/2-Closed	1.18	7.4
3/4-Closed	1.97	12.2

Small deviations in position, corresponding to a "statistical" 10–20% variation in area of the openings, would not contribute significantly to process variability. Improperly positioned stoppers equivalent to the 1/2-closed or 3/4-closed, do significantly affect freeze drying, the effect being much more serious for the smaller stoppers. A 12% increase in drying time (Table X) might well result in product loss when the shelf temperature is increased for secondary drying at the end of the *expected* primary drying time.

"Effects of Product Resistance Variation"—The dried product resistance is the major mass transfer barrier in freeze drying, and therefore, interval variations in product resistance would have a significant impact on process variability, provided some mechanism exists which produces intervial variations in product resistance. Potentially, the variation in freezing behavior is such a mechanism. Not all vials in a dryer freeze at the same time nor is the degree of supercooling the same for all vials. Thus, there is a distribution of freezing behavior in any given lot. Order of magnitude changes in freezing rate may produce differences in $\bar{R}_p$ as large as a factor of 2. Greater supercooling and faster freezing results in smaller ice crystals, with correspondingly smaller pores in the dried product, yielding greater resistance to vapor flow (4). The effect of small variations in freezing behavior has not been systematically studied. The reproducibility of resistance data generated with the microbalance technique suggests that the natural variation in freezing behavior characteristic of the microbalance "fast freeze" procedure produces variations in resistance on the order of 5%. One might expect the slower freeze characteristic of a vial process to be somewhat more reproducible. Indeed, for the only system we have studied in detail (an amorphous antibiotic), the standard deviation in product resistance is less than about 1% for vial samples but is about 5% for microbalance samples.

By calculating the effects on drying time and product temperature of a given arbitrary change in product resistance parameters R_0 and A_1 (Eq. 12), the process variability arising from product resistance variability is evaluated. A 10% standard deviation in resistance produces

TABLE XI. Effect of Nonuniform Drying on Cycle Design: Process Optimization Results[a]

P_c (mm Hg)	Control Temperature, °C	Mean *TD*	Delay (% of Mean *TD*)	Total Primary Cycle (hr)
		5% PVP Resistance, −25 °C Collapse Temperature		
0.05	−25.85	18.8	16.9	22.0
0.10	−25.67	20.3	15.6	23.5
0.20	−25.50	26.9	16.6	31.4
0.30	−25.36	42.0	18.0	49.6
		5% Mannitol Resistance, −15 °C Collapse Temperature		
0.05	−15.96	16.7	18.7	19.8
0.10	−15.80	16.9	16.9	19.7
0.20	−15.74	18.3	17.5	21.5
0.30	−15.71	20.2	18.9	24.0

[a] Calculations for 8 ml fill volume in 5816W vials loaded directly on the pilot dryer shelf.

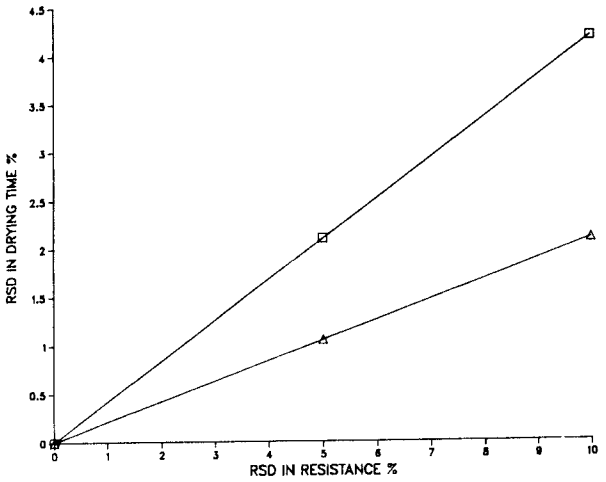

Figure 13—Effect of nonuniformity in product resistance on primary drying time: chamber pressure 0.1 mmHg; 8 ml fill volume; 5816W vials; sublimation temperature (average vial), −25 °C: △, 5% (v/v) *PVP*; □, 5% (w/w) mannitol.

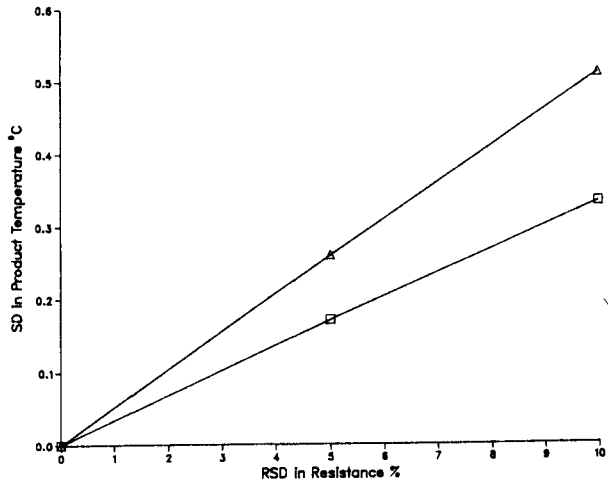

Figure 14—Effect of nonuniformity in product resistance on product temperature: chamber pressure 0.1 mmHg; 8 ml fill volume; 5816W vials; sublimation temperature (average vial), −25 °C: △, 5% (v/v) *PVP*; □, 5% (w/w) mannitol.

about a 4.5% standard deviation for mannitol drying time but only a 2% standard deviation for *PVP* (Fig. 13). Note that mannitol has a much higher product resistance than does *PVP*. Even for a 10% standard deviation in product resistance, the standard deviation in product temperature (Fig. 14) is relatively small (≈0.5 °C for *PVP* and ≈0.3 °C for mannitol).

3.5 Process optimization

Process optimization calculations are illustrated for two hypothetical products freeze dried in 5816W vials with a fill volume of 8 ml. One product is assumed to have the resistance behavior of 5% *PVP* with a collapse temperature of −25 °C while the other has the resistance characteristics of 5% mannitol and a collapse temperature of −15 °C. Our objective is the most efficient process possible, constrained by a product loss less than 0.05%. It is arbitrarily assumed that a loss of 0.05% (10 vials out of 20,000) through excessive heat input at some stage of the process is acceptable. Although far from rigorous, we assume that, as a first approximation, the product temperatures and drying rates follow a normal distribution. Thus, 99.95% of the vials freeze dry within $3.285\sigma(t)$ degrees of the mean temperature, where $\sigma(t)$ is the standard deviation in product temperature. For purposes of this illustration, it is assumed that the only significant components of the variance in product temperature are variation in shelf surface temperature and vial heat transfer coefficient variability, where these components of variance are evaluated as outlined in the previous section of this report. The data in Tables VIII and IX, as well as corresponding data for 5% mannitol freeze dried at −15°, are used to evaluate $\sigma(t)$, and the temperature safety margin, $3.285\ \sigma(t)$, is determined. The desired control temperature for the average vial is then $3.285\ \sigma(t)$ degrees lower than the collapse temperature. The FDRYT version of the program is then run to determine, for each chamber pressure of interest, the sequence of shelf fluid temperatures needed to maintain the average product temperature at the control temperature and to determine the mean drying time. The delay time is the difference between the time required to complete drying for 99.95% of the vials and the mean drying time. The delay time is evaluated as described by Eq. 47. The required value of $\sigma(TD)$ is evaluated as outlined in the previous section, again assuming that shelf temperature variability and vial heat transfer coefficient variability are the only components of the variance in drying time, *TD*.

The calculated results (Table XI) show that the most efficient process is one which uses a relatively low chamber pressure. The total primary drying time for the "*PVP*-like" product increases as the chamber pressure increases for all chamber pressures studied; while the drying time for the "mannitol-like" product actually passes through a shallow minimum around a chamber pressure of 0.1 mmHg. While the drying time is not particularly sensitive to chamber pressure between 0.05 and 0.1 mmHg for either product, clearly use of high chamber pressure should be avoided. As discussed previously, the increase in drying time one observes with increases in chamber pressure *at constant product temperature* reflects the decrease in the driving force for vapor flow.

It should be noted that the calculated temperature safety margins are relatively small, less than 1 °C in all cases. In a real freeze-drying run where measured product temperature is used to control heat input and maintain the control temperature, the safety margin would need to be increased to allow for experimental error in the measured mean temperature. However, in the absence of gross deviations from a normal distribution or gross systemic errors in measured temperature, the required safety margin is not likely to be greater than 2 °C. Expressed as a percentage of mean drying time, the delay times are all in the 15%–19% range. Again, if in actual freeze-drying practice the mean drying time is determined by product temperature response, the delay times would need to be increased somewhat to reflect experimental uncertainty in the measured mean drying time. However, assuming temperature output from at least five vials is used and no significant systematic errors exist, the required adjustment to delay time is negligible for a normal distribution of sublimation rates.

For the sources of process nonuniformity considered here, the deviations from a normal distribution are probably not serious enough to invalidate the general conclusions reached. However, improperly positioned closures or abnormal heat transfer due to spills coating the vials with solution are two examples of variability clearly outside the range of application of the calculations presented here.

4. Conclusions

Theoretical concepts are used to properly define key heat and mass transfer coefficients which can then be experimentally determined in laboratory experiments as a function of the relevant variables. Steady-state transport theory is employed to relate freeze-drying properties in a thermodynamic sense. That is, the theoretical relations relate measurable quantities, such as sublimation rate and product temperature. Once the necessary transport coefficients are available from experiments, or estimated from correlations based on experimental data, the transport equations are solved with a computer under the conditions of interest to generate a computer-simulated freeze-drying "experiment". Thus, sublimation rates, temperatures and pressures as a function of time are predicted for trial processes not studied experimentally. The theoretical model may also be used to estimate the effects of known variability in process conditions (shelf temperature variation, variability in vial heat transfer) on the freeze-drying process.

Once the heat and mass transfer parameters for the containers and freeze dryers of interest are measured, or estimated, the only additional data required to initiate computer freeze-drying studies on a new product are the collapse (or eutectic) temperature of the product and the dried product resistance as a function of the thickness of the dried product layer. While at present these properties cannot be quantitatively estimated, the appropriate experimental studies normally require only a few days and a small amount of material (at a minimum, the equivalent of the fill volume for one vial). Not only can process development proceed very quickly with computer freeze-drying studies, but the effects of equipment differences can be predicted (i.e., vials on a tray bottom vs. vials directly on the shelf; effect of different shelf heat transfer coefficient, etc.). Thus, scale-up problems can be minimized. While in our experience, the computer calculations are quite accurate and can replace most of the trial and error experimental work in development, computer freeze drying should not be viewed as a replacement for all experimental development studies. Rather, there is still a need for limited pilot scale studies to confirm, or perhaps refine, the theoretical results. Finally, when a process is first introduced into production use, it is always wise to proceed with caution. For example, one should use a slightly larger temperature safety margin than believed necessary in determining the control temperature, and a longer delay time than that estimated should be used. Thus, although not a complete replacement for more conventional development studies, the combination experimental-theoretical approach described in this report can be very useful in the development and scale-up of optimum processes for the freeze drying of pharmaceuticals.

Appendix

A listing of the computer programs used, written in "MLAB", are given in this section. Table XII gives the MLAB equivalent of the symbols defined in the text for those cases where the symbols are different.

FDFN.DAT

```
00100  DM__LIST(0,0)';
00200  FUNCTION G1(D)=(SRP(D)/AP+RS(D)
       +RT(D))*M-PC(I);
00300  FUNCTION G2(D)=IF T1<1000 THEN
       RS(D)*M-PV+PTR ELSE RS(D)*M-
       PV+PC(I);
00400  FUNCTION G3(D)=IF T1<1000 THEN
       RT(D)*M-PTR+PC(I) ELSE PC(I)-PTR;
00500  FUNCTION G4(D)=0.1833*M*(1/
       (AV*KV(D))+1/(ATV*KT(D)+ (LM-L)/
       (AP*KI))-TS(I)+T;
00600  FUNCTION G5(D)=0.1833*M/
       (AV*KV(D))-TT+TB;
00700  FUNCTION G6(D)=IF KTC<1 THEN
       0.1833*M/(ATV*KT(D))-TS(I)+TT ELSE
       TT-TS(I);
00750  FUNCTION TED(D)=T+(TB-T)*KR;
```

TABLE XII. Identification of Symbols Used in the MLAB Computer Programs

Text Symbol	Symbol Meaning	MLAB Symbol
$\hat{R}_p$	Normalized dried product resistance	SRP (D)
R_s	Stopper (closure) resistance	RS (D)
R_{tr}	Tray lid resistance	RT (D)
K_v	Vial heat transfer coefficient	KV (D)
K_{tr}	Tray heat transfer coefficient	KT (D)
K_I	Effective product thermal conductivity	KI
R_0	Product resistance parameter (Eq. 12)	R0
A_1	Product resistance parameter (Eq. 12)	A1 (D)
A_2	Product resistance parameter (Eq. 12)	A2 (D)
A_v	Vial area (from OD)	AV
A_p	Cross-sectional area of product	AP
l	Thickness of dried product	L
l_m	Maximum thickness of dried product	LM
$\dot{m}$	Sublimation rate, ghr^{-1}	M
P_0	Equilibrium vapor pressure of subliming ice (mmHg)	P0 (D)
P_v	Pressure in the vial (mmHg)	PV
P_{tr}	Pressure inside the tray (mmHg)	PTR
P_c	Chamber pressure	PC (I)
T_b	Product temperature, bottom center of vial (°K)	TB
T_t	Tray bottom temperature (°K)	TT
T_s	Shelf surface temperature (°K)	TS (I), TS
T_E	Product temperature, bottom edge (°K)	TED (D)
K_R	Radial heat flow coefficient	KR
Δl	Increment in l during one stage of computer solution	DL
TD	Primary drying time (hr)	TDRY
ϵ	Volume fraction of ice in product	E

```
00800 FUNCTION P0(D)=2.6983@10*EXP
      (-6144.96/T);
00900 FUNCTION SRP(D)=R0+A1(D)*L/
      (1+A2(D)*L);
01000 FUNCTION RS(D)=IF T1<1000 THEN
      1/(S0+S1*(PV+PTR)*.5) ELSE
      1/(S0+S1*(PV+PC(I))*.5);
01100 FUNCTION RT(D)=
      1/(T0+T1*(PTR+PC(I))*.5);
01200 FUNCTION KV(D)=IF T1<1000 THEN
      KC+KP*PTR/(1+KD*PTR) ELSE
      KC+KP*PC(I)/(1+KD*PC(I));
01300 FUNCTION KT(D)=KTC
      +KTP*PC(I)/
      (1+KTD*PC(I));
01400 CONSTRAINTS POS;!M>0;!T<TC;
      !PTR>0;!PV>0;
```

FDRY.DAT

```
00100 LM__1.089*V/AP;
00200 TS__ST+273.16;
00300 DL__LM/5;
00400 FOR N__0:4 DO(DO SOLN);
00500 QT ROW 1__Q ROW 1;
00600 QT ROW 2__Q1 ROW 1;
00700 QT ROW 3__Q ROW 2;
00800 QT ROW 6__Q1 ROW 2;
00900 QT ROW 5__Q ROW 3;
01000 QT ROW 6__Q1 ROW 3;
01100 QT ROW 7__Q ROW 4;
01200 QT ROW 8__Q1 ROW 4;
01300 QT ROW 9__Q ROW 5;
01400 QT ROW 10__Q1 ROW 5;
01500 P(1,1)__0;
01600 P(2,1)__Q1(1,8);
01700 P(3,1)__P(2,1);
01800 P(4,1)__P(3,1)+Q1(2,8);
01900 P(5,1)__P(4,1);
02000 P(6,1)__P(4,1)+Q1(3,8);
02100 P(7,1)__P(6,1);
02200 P(8,1)__P(7,1)+Q1(4,8);
02300 P(9,1)__P(8,1);
02400 P(10,1)__P(9,1)+Q1(5,8);
02500 TDRY__P(10,1);
02600 LRES COL 1__QT COL 1;
02700 LRES COL 2__QT COL 9;
02800 LRES COL 3__QT COL 10;
02900 LRES COL 4__QT COL 11;
03000 LRES COL 5__QT COL 12;
03100 TPRESS COL 1__P;
03200 TPRESS COL 2__QT COL 13;
03300 TPRESS COL 3__QT COL 3;
03400 TPRESS COL 4__QT COL 4;
03500 TPRESS COL 5__LIST(PC(1),PC(1),PC(2),
      PC(2),PC(3),PC(3),
      PC(4),PC(4),PC(5),PC(5));
03600 TTEMP COL 1__P;
03700 TTEMP COL 2__LIST(ST(1),ST(1),ST(2),
      ST(2),ST(3),ST(3),
      ST(4),ST(4),ST(5),ST(5));
03800 TTEMP COL 3__QT COL 5;
03900 TTEMP COL 4__QT COL 14;
04000 TTEMP COL 5__QT COL 6;
04100 TTEMP COL 6__QT COL 7;
04200 RATE COL 1__P;
04300 RATE COL 2__QT COL 1;
04400 RATE COL 3__QT COL 2;
04500 RATE COL 4__QT COL 6;
04600 RATE COL 5__QT COL 7;
04700 RATE COL 6__QT COL 15;
04800 TYPE "COMPUTER FREEZE DRYING:
      FIXED CHAMBER PRESSURE AND
      SHELF TEMPERATURE";
04900 TYPE "INPUT DATA";
05000 TYPE E,V,ST &' PC;
05100 TYPE "PRIMARY DRYING TIME
      (HOURS)";
05200 TYPE TDRY;
05300 TYPE "RESISTANCE VS L";
05400 TYPE "L  RP  RS  RTR  RTOTAL";
05500 TYPE LRES;
05600 TYPE "RESISTANCE VS L PLOT;
```

```
        A=RP,B=RS,C=RTR,D=RTOTAL";
05700   TTYDRAW LRES;
05800   TYPE "PRESSURE VS TIME";
05900   TYPE "TIME P0 PV PTR PC";
06000   TYPE TPRESS;
06100   TYPE "PRESSURE VS TIME PLOT;
        A=P0,B=PV,C=PTR,D=PC";
06200   TTYDRAW TPRESS;
06300   TYPE "TEMPERATURE VS TIME";
06400   TYPE "TIME SHELF T TRAY T TBE TB
        TSUB";
06500   TYPE TTEMP;
06600   TYPE "TEMPERATURE VS TIME PLOT;
        A=SHELF, B=TRAY, C=TBE,D=TB,
        E=TSUB";
06700   TTYDRAW TTEMP;
06800   TYPE "TIME, L, RATE,
        TEMPERATURES,DEVIATIONS";
06900   TYPE "TIME L RATE TB TSUB
        DEV";
07000   TYPE RATE;
07100   TYPE " **************************";
```

SOLN.DAT

```
00100   L__N*DL;
00200   I__N+1;
00300   M__V/20;
00400   PTR__PC(I)+.1;
00500   PV__PTR+.1;
00600   TT__TS(I)-10;
00700   T__TC-10;
00800   TB__T+1;
00900   SILENT FIT(M,PV,PTR,TT,TB,T),G1 TO
        DM,G2 TO DM,G3 TO DM,G4 TO DM,G5
        TO DM,G6 TO DM;
01000   !POS;
01100   !50;
01200   !;
01400   Q(I,1)__L;
01500   Q(I,2)__M;
01600   Q(I,3)__PV;
01700   Q(I,4)__PTR;
01800   Q(I,5)__TT-273.16;
01900   Q(I,6)__TB-273.16;
02000   Q(I,7)__T-273.16;
02200   Q(I,9)__SRP(0)/AP;
02300   Q(I,10)__RS(0);
02400   Q(I,11)__RT(0);
02500   Q(I,12)__Q(I,9)+Q(I,10)+Q(I,11);
02600   Q(I,13)__P0(0);
02700   Q(I,14)__TED(0)-273.16;
02800   Q(I,15)__SQRT(G1(0)^2+G2(0)^2+G-
        3(0)^2+G4(0)^2+G5(0)
        ^2+G6(0)^2);
02900   L__(N+1)*DL;
03000   SILENT FIT (M,PV,PTR,TT,TB,T), G1 TO
        DM,G2 TO DM, G3 TO DM,G4 TO DM,G5
        TO DM,G6 TO DM;
03100   !POS;
03200   !50;
03300   !;
03400   Q1(I,1)__L;
03500   Q1(I,2)__M;
03600   Q1(I,3)__PV;
03700   Q1(I,4)__PTR;
03800   Q1(I,5)__TT-273.16;
03900   Q1(I,6)__TB-273.16;
04000   Q1(I,7)__T-273.16;
04100   Q1(I,8)__1.836*DL*AP*E/(Q(I,2)+Q1(I,2));
04200   Q1(I,9)__SRP(0)/AP;
04300   Q1(I,10)__RS(0);
04400   Q1(I,11)__RT(0);
04500   Q1(I,12)__Q1(I,9)+Q1(I,10)+Q1(I,11);
04600   Q1(I,13)__P0(0);
04700   Q1(I,14)__TED(0)-273.16;
04800   Q1(I,15)__SQRT(G1(0)^2+G2(0)
        ^2+G3(0)^2+G4(0)^2+G5(0)^
        2+G6(0)^2);
```

FDFNT.DAT

```
00100   DM__LIST(0,0)';
00200   FUNCTION G1(D)=(SRP(D)/AP+RS(D)
        +RT(D))*M-P0(D)+PC(I);
00300   FUNCTION G2(D)=IF T1<1000 THEN
        RS(D)*M-PV+PTR ELSE RS(D)
        *M-PV+PC(I);
00400   FUNCTION G3(D)=IF T1<1000 THEN
        RT(D)*M-PTR+PC(I) ELSE PC(I)-PTR;
00500   FUNCTION G4(D)=0.1833*M*(1/
        (AV*KV(D))+1/(ATV*KT(D))+
        (LM-L)/(AP*KI))-TS+T;
00600   FUNCTION G5(D)=0.1833*M/
        (AV*KV(D))-TT+TB;
00700   FUNCTION G6(D)=IF KTC<1 THEN
        0.1833*M/(ATV*KT(D))-TS+TT ELSE
        TT-TS;
00750   FUNCTION TED(D)=T+(TB-T)*KR;
00800   FUNCTION P0(D)=2.6983@10*EXP
        (-6144.96/T);
00900   FUNCTION SRP(D)=R0+A1(D)*L/
        (1+A2(D)*L);
01000   FUNCTION RS(D)=IF T1<1000 THEN
        1/(S0+S1*(PV+PTR)*.5) ELSE
        1/(S0+S1*(PV+PC(I))*.5);
01100   FUNCTION RT(D)=
        1/(T0+T1*(PTR+PC(I))*.5);
01200   FUNCTION KV(D)=IF T1<1000 THEN
        KC+KP*PTR/(1+KD*PTR) ELSE
        KC+KP*PC(I)/(1+KD*PC(I));
01300   FUNCTION KT(D)=KTC+KTP*PC(I)/
        (1+KTD*PC(I));
01400   CONSTRAINTS P0S;!M>0;!TS>TT;
        !TT>TB;!TB>T;!PTR>0;!PV>PTR;
```

FDRYT.DAT

```
00100   LM__1.089*V/AP;
00300   DL__LM/5;
00400   FOR N__0:4 DO(DO SOLNT);
00500   QT ROW 1__Q ROW 1;
00600   QT ROW 2__Q1 ROW 1;
```

```
00700  QT ROW 3__Q ROW 2;
00800  QT ROW 4__Q1 ROW 2;
00900  QT ROW 5__Q ROW 3;
01000  QT ROW 6__Q1 ROW 3;
01100  QT ROW 7__Q ROW 4;
01200  QT ROW 8__Q1 ROW 4;
01300  QT ROW 9__Q ROW 5;
01400  QT ROW 10__Q1 ROW 5;
01410  ST__QT COL 16;
01500  P(1,1)__0;
01600  P(2,1)__Q1(1,8);
01700  P(3,1)__P(2,1);
01800  P(4,1)__P(3,1)+Q1(2,8);
01900  P(5,1)__P(4,1);
02000  P(6,1)__P(4,1)+Q1(3,8);
02100  P(7,1)__P(6,1);
02200  P(8,1)__P(7,1)+Q1(4,8);
02300  P(9,1)__P(8,1);
02400  P(10,1)__P(9,1)+Q1(5,8);
02500  TDRY__P(10,1);
02600  LRES COL 1__QT COL 1;
02700  LRES COL 2__QT COL 9;
02800  LRES COL 3__QT COL 10;
02900  LRES COL 4__QT COL 11;
03000  LRES COL 5__QT COL 12;
03100  TPRESS COL 1__P;
03200  TPRESS COL 2__QT COL 13;
03300  TPRESS COL 3__QT COL 3;
03400  TPRESS COL 4__QT COL 4;
03500  TPRESS COL 5__LIST (PC(1),PC(1),PC(2),
       PC(2),PC(3),
       PC(3),PC(4),PC(4),PC(5),PC(5));
03600  TTEMP COL 1__P;
03700  TTEMP COL 2__ST;
03800  TTEMP COL 3__QT COL 5;
03900  TTEMP COL 4__QT COL 14;
04000  TTEMP COL 5__QT COL 6;
04100  TTEMP COL 6__QT COL 7;
04200  RATE COL 1__P;
04300  RATE COL 2__QT COL 1;
04400  RATE COL 3__QT COL 2;
04500  RATE COL 4__QT COL 6;
04600  RATE COL 5__QT COL 7;
04700  RATE COL 6__QT COL 15;
04710  CYCLE COL 1__P;
04720  CYCLE COL 2__LIST (PC(1),PC(1),PC(2),
       PC(2),PC(3),PC(3),
       PC(4),PC(4),PC(5),PC(5));
04730  CYCLE COL 3__ST;
04800  TYPE "COMPUTER FREEZE DRYING:
       FIXED CHAMBER PRESSURE AND SUB
       TEMP";
04900  TYPE "INPUT DATA";
05000  TYPE E,V,T;
05010  TYPE "FREEZE DRYING CYCLE";
05020  TYPE "TIME  PC  SHELF T";
05030  TYPE CYCLE;
05100  TYPE "PRIMARY DRYING TIME
       (HOURS)";
05200  TYPE TDRY;
05300  TYPE "RESISTANCE  VS  L";
05400  TYPE "L  RP  RS  RTR  RTOTAL";
05500  TYPE LRES;
05600  TYPE "RESISTANCE VS L PLOT;
       A=RP,B=RS,C=RTR,D=RTOTAL";
05700  TTYDRAW LRES;
05800  TYPE "PRESSURE  VS  TIME";
05900  TYPE "TIME  P0  PV  PTR  PC";
06000  TYPE TPRESS;
06100  TYPE "PRESSURE VS TIME PLOT;
       A=P0,B=PV,C=PTR,D=PC";
06200  TTYDRAW TPRESS;
06300  TYPE "TEMPERATURE VS  TIME";
06400  TYPE "TIME  SHELF T  TRAY
       T  TBE  TB  TSUB";
06500  TYPE TTEMP;
06600  TYPE "TEMPERATURE VS TIME PLOT;
       A=SHELF, B=TRAY, C=TBE,D=TB,
       E=TSUB";
06700  TTYDRAW TTEMP;
06800  TYPE "TIME, L, RATE,TEMPERATURES,
       DEVIATIONS";
06900  TYPE "TIME L RATE TB TSUB DEV";
07000  TYPE RATE;
```

SOLNT.DAT

```
00100  L__N*DL;
00200  I__N+1;
00300  M__V/20;
00400  PTR__PC(I)+.1;
00500  PV__PTR+.1;
00600  TB__T+1;
00700  TT__TB+10;
00800  TS__TT+10;
00900  SILENT FIT (M,PV,PTR,TT,TB,TS),G1 TO
       DM,G2 TO DM,G3 TO DM,G4 TO DM,G5
       TO DM,G6 TO DM;
01000  !POS;
01100  !50;
01200  !;
01400  Q(I,1)__L;
01500  Q(I,2)__M;
01600  Q(I,3)__PV;
01700  Q(I,4)__PTR;
01800  Q(I,5)__TT-273.16;
01900  Q(I,6)__TB-273.16;
02000  Q(I,7)__T-273.16;
02200  Q(I,9)__SRP(0)/AP;
02300  Q(I,10)__RS(0);
02400  Q(I,11)__RT(0);
02500  Q(I,12)__Q(I,9)+Q(I,10)+Q(I,11);
02600  Q(I,13)__P0(0);
02700  Q(I,14)__TED(0)-273.16;
02800  Q(I,15)__SQRT (G1(0)
       ^2+G2(0)^2+g3(0)^2+G4(0)
       ^2+G5(0)^2+G6(0)^2);
02900  L__(N+1)*DL;
02910  Q(I,16)__TS-273.16;
03000  SILENT FIT(M,PV,PTR,TT,TB,TS),G1 TO
```

```
      DM,G2 TO DM,G3 TO DM,G4 TO DM,G5
      TO DM,G6 TO DM;
03100 !POS;
03200 !50;
03300 !;
03400 Q1(I,1)__L;
03500 Q1(I,2)__M;
03600 Q1(I,3)__PV;
03700 Q1(I,4)__PTR;
03800 Q1(I,5)__TT-273.16;
03900 Q1(I,6)__TB-273.16;
04000 Q1(I,7)__T-273.16;
04100 Q1(I,8)__1.836*DL*AP*E/(Q(I,2)+Q1(I,2));
04200 Q1(I,9)__SRP(0)/AP;
04300 Q1(I,10)__RS(0);
04400 Q1(I,11)__RT(0);
04500 Q1(I,12)__Q1(I,9)+Q1(I,10)+Q1(I,11);
04600 Q1(I,13)__P0(0);
04700 Q1(I,14)__TED(0)-273.16;
04800 Q1(I,15)__SQRT(G1(0)^2+G2(0)
      ^2+G3(0)^2+G4(0)^2+G5(0)^2+G6(0)
      ^2);
04810 Q1(I,16)__TS-273.16;
```

References

1. Jennings, T. A., "Optimization of the Lyophilization Schedule," *Drug Cosmet. Ind.*, **127,** 43 (1980).
2. Pikal, M. J., Lukes, A. L., and Lang, J. E., "Thermal Decomposition of Amorphous β-Lactam Antibacterials," *J. Pharm. Sci.*, **66,** 1312 (1977).
3. MacKenzie, A. P., "Principles of Freeze-Drying," *Transplantation Proc., Suppl. 1*, **VIII**(2), 181 (1976).
4. Pikal, M. J., Shah, S., Senior, D., and Lang, J. E., "Physical Chemistry of Freeze-Drying: Measurement of Sublimation Rates for Frozen Aqueous Solutions by a Microbalance Technique," *J. Pharm. Sci.*, **72,** 635 (1983).
5. Pikal, M. J., Roy, M. L., and Shah, S., "Critical Factors in the Development of Freeze Drying Processes," *IPT Symposium on Small Volume Parenterals*, 129th APhA Annual Meeting, Las Vegas, Nevada, Vol. 12, No. 1, 1982.
6. Patel, R. M., and Hurwitz, A., "Eutectic Temperature Determination of Preformulation Systems and Evaluation by Controlled Freeze Drying," *J. Pharm. Sci.*, **61,** 1806 (1972).
7. Gatlin, L., and Deluca, P., "A Study of the Phase Transitions in Frozen Antibiotics Solutions by Differential Scanning Calorimetry," *J. Parenteral Drug Assoc.*, **34,** 398 (1980).
8. Jennings, T. A., "The Effect of Resistivity Probe Design on the Measurement of the Freezing Temperature of Lyophilized Formulations," *J. Parenteral Drug Assoc.*, **34,** 109 (1980).
9. MacKenzie, A. P., "Factors Affecting the Mechanism of Transformation of Ice Into Water Vapor in the Freeze-Drying Process," *Ann. N.Y. Acad. Sci.*, **125,** 522 (1965).
10. King, C. J., "Freeze Drying of Foods," CRC Press, Cleveland, Ohio, 1971.
11. Mellor, J. D., "Fundamentals of Freeze Drying," Academic Press, New York, 1978.
12. Burghart, M. D., and Bowley, W. W., "Sublimation in a Porous Continuum Developed from Nonequilibrium Thermodynamics," *J. Heat Transfer, Trans. ASME*, **96,** 319 (1974).
13. Tsvetkov, T. D., and Vulchanov, N. L., "Toward the Mathematical Modeling of Heat and Mass Transfer in Vacuum Freeze-Drying. I. Thermodynamic Analysis of Heat and Mass Transfer Processes in Capillary Porous Materials Undergoing Freeze Drying," *Cryobiology*, **18,** 155 (1981).
14. Liapis, A. I., and Litchfield, R. J., "Optimal Control of A Freeze Dryer—I. Theoretical Development and Quasi Steady State Analysis," *Chem. Eng. Sci.*, **34,** 975 (1979).
15. Litchfield, R. J., and Liapis, A. I., "Some Guidelines for the Desirable Design and Operation of Freeze-Dryers," AIChE Summer National Meeting, Cleveland, Ohio, 1982.
16. DeGroot, S. R., and Mazur, P., "Non-Equilibrium Thermodynamics," North Holland, Amsterdam, 1963.
17. Dushman, S., and Lafferty, J. M., "Scientific Foundations of Vacuum Technique," John Wiley and Sons, Inc., New York, 2nd Ed., 1962.
18. Nail, S. L., "The Effect of Chamber Pressure on Heat Transfer in the Freeze Drying of Parenterals Solutions," *J. Parenteral Drug Assoc.*, **34,** 358 (1980).
19. Pikal, M. J., Roy, M. L., and Shah, S., "Mass and Heat Transfer in Vial Freeze-Drying of Pharmaceuticals: Role of the Vial," *J. Pharm. Sci.*, **73,** 1224 (1984).
20. Cise, M. D., "Freeze-Drying Cycle Design: Effects of Process Physics," AIChE Summer National Meeting, Cleveland, Ohio, 1982.
21. Pikal, M. J., and Dellerman, K. M., unpublished observations.
22. MacKenzie, A. P., and Luyet, B. J., "Apparatus for the Automatic Recording of Freeze-Drying Rates at Controlled Specimen Temperatures," *Biodynamica*, **9,** 193 (1964).
23. Ho, N. F., and Roseman, T. J., "Lyophilization of Pharmaceutical Injections: Theoretical Physical Model," *J. Pharm. Sci.*, **68,** 1170 (1979).
24. Barrer, R. M., "Diffusion in Porous Media," *Appl. Materials Res.*, **2,** 129 (1963).
25. Pikal, M. J., and Shah, S., unpublished observations.
26. Partington, J. R., "An Advanced Treatise on Physical Chemistry," Vol. 1, John Wiley and Sons, New York, 1949, p. 891.
27. Perry, J. H., "Chemical Engineers Handbook," 4th Edition, McGraw-Hill Book Co., New York, 1963.

Resumen: El desarrollo de los procesos de liofilización tiene lugar, comúnmente, por intermedio de un enfoque experimental empírico basado en tanteos. Esto comsume mucho tiempo y la extrapolación a los equipos de producción no tiene un alto grado de confiabilidad. Este trabajo describe el uso de la teoría fenomenológica, en el que los estudios de laboratorio sirven para determinar los parámetros clave, usados para guiar el programa de experimentos encaminados a optimizar el estadio primario de secado de un proceso, para una combinación dada de producto y envase. La descripción teórica del secado primario incluye el problema de combinación de transmisión de calor y de materia, lo cual puede ser descripto en forma satisfactoria usando un modelo de estado estacionario en donde el flujo de calor está dado por el producto del flujo de la materia y el calor de sublimación. En general, uno encuentra tres vallas o resistancias en el transporte de la materia: la resistencia ofrecida por la capa del producto seco, la resistencia que presenta el tubito semi-tapado y la resistencia de la cámara. La resistencia se define como la relación de la differencia de presión sobre el flujo de la materia, y se la determina en forma experimental para cada barrera. Normalmente, la resistencia del producto seco aumenta con el tiempo, conjuntamente con el aumento del espesor de producto seco y, en la mayoría de los casos, es responsable por el 90% de la resistencia total al transporte de la materia. Tres barreras impiden el flujo de calor de la superficie del estante al hielo que está sublimando. Estas son: la interface entre la superficie del estante y el fondo de la bandeja que se usa para colocar las botellitas, la interface entre la superficie de la bandeja y la base de las botellitas, y el hielo que se encuentra entre el fondo de las